NOTE TO USERS

This reproduction is the best copy available.

UMI®

University of Alberta

Roles of L-type Calcium Currents and 5-HT in Motoneurons of Chronic Spinal Rats

by

Xiaole Li 

A thesis submitted to the Faculty of Graduate Studies and Research in partial fulfillment of the requirements for the degree of Master of Science.

Centre for Neuroscience

Edmonton, Alberta
Fall 2005

ABSTRACT

After long-term spinal cord transection, motoneurons in rat spinal cords exhibit large sodium and calcium persistent inward currents (PICs), which are responsible for the muscle spasticity after chronic injury. The persistent calcium currents are mediated by low threshold L-type calcium channels (Ca PIC). This thesis demonstrates that the Ca currents are capable of activating calcium-activated small conductance potassium channels (SK channel), which are apamin sensitive and subsequently produce an outward current that counteracts the L-type calcium currents and results in a smaller recorded net Ca PIC. Our study also shows that the calcium channels become supersensitive to 5-HT after chronic spinal cord injury and can be facilitated with very low dose 5-HT (1μM). In normal rats, high dose (30μM) 5-HT are needed to facilitate the Ca PIC. We suggest that residual 5-HT in spinal cord after injury acts on supersensitive receptors to produce the large Ca PICs seen in chronic spinal rats.

ACKNOWLEDGEMENTS

I would like to express my appreciation and gratitude to my supervisor, Dr. David J. Bennett, and to my advisory committee members, Drs. Peter Smith and Kelvin Jones. Their valuable advice benefited me throughout my graduate studies.

A thank-you also to Yunru Li and Philip Harvey for the help they gave to me. Special thanks to Leo Sanelli for his expert technical assistance and to Dr. Monica Gorassini for her helpful and constructive suggestion in my research.

LIST OF CONTENTS

LIST OF TABLES

LIST OF FIGURES

LIST OF ABBREVIATIONS

5-HT	5-hydroxytryptamine (serotonin)
ACSF	artificial cerebrospinal fluid
AHP	afterhyperpolarization
Ca PIC	calcium persistent inward current
Ca_V	voltage-gated calcium channel
F	frequency
I	current
I_{end}	cessation of firing on descending current ramp
I_{on}	initiation of firing on ascending current ramp
mACSF	modified ACSF
Na PIC	sodium persistent inward current
nACSF	normal ACSF
NE	norepinephrine
NSR	negative slope region
PIC	persistent inward current
Rm	membrane input resistance
S	Sacral
SK	small conductance calcium-activated potassium current
TTX	tetrodotoxin
V	voltage
Vm	resting membrane potential
V_{on}	PIC voltage onset
V_{th}	spike voltage threshold

Chapter 1: Introduction

Spasticity and Spinal Cord Injury

A comprehensive definition of spasticity is difficult to give, largely due to the presently insufficient knowledge of the neurobiology of this complex motor disorder that appears with many injuries to the brain or spinal cord (Young 1994). Lance defined spasticity as a velocity-dependent increase in tonic stretch reflexes with exaggerated tendon jerks, caused by the hyperexcitability of the stretch reflex (Lance and Burke 1974), which is a restrictive but widely quoted definition of spasticity. This definition is appropriate for describing spasticity that results from brain injury such as stroke, but does not very well characterize spasticity that follows spinal cord injury, which is much more irregular, with cutaneously evoked muscle spasms being the hallmark (Kuhn and Macht 1948). More than 80% of spinal cord injury patients develop a spasticity syndrome, which is clinically characterized as muscle hyperreflexia, hypertonus, clonus and spasms (Levi et al. 1995). The spasms usually develop in weeks or months after the spinal cord injury, and involves extensive extensor and/or flexor muscle contractions that last from seconds to minutes, and are triggered by only transient non-noxious stimuli (Kuhn and Macht 1948). Spasticity usually causes gait, movement, and bladder dysfunction, as well as pain (Ashby et al. 1987; Bennett et al. 1999a; Heckman 1994; Taylor et al. 1997). It has classically been assumed that these syndromes are caused by lesions of the corticospinal tracts, but it is actually unknown which descending motor tracts are responsible for each symptom (Young 1994), and it is becoming clear that the loss of brainstem 5-HT tracts plays a central role, as we described below (see also Harvey et al. 2005a,b,c). Conventional therapies are usually not effective in treating the spasticity in these patients,

partly due to the lack of understanding of the underlying mechanisms of spasticity (Little et al. 1989).

Most of the clinical symptoms of spasticity are related to long lasting reflexes, triggered by polysynaptic reflexes and ultimately leading to sustained muscle spasms. For example, these include increased tonic stretch reflexes (Thilmann et al. 1991) and cutaneous/flexor reflexes (Bennett et al. 1999a). Previous studies indicate that the intrinsic excitability of motoneurons is profoundly increased over the months following spinal cord injury, and this plays a major role in the generation of spasticity, in both rats (Bennett et al. 2001b) and humans (Gorassini et al. 2004). That is, a brief stimulation can trigger long lasting firing by activating voltage-dependent persistent inward currents (PICs), which can cause a sustained depolarization (plateau potential) and firing that outlasts the stimulation by many seconds. These PICs/plateaus can be triggered by brief dorsal root stimulation, and then produce prolonged reflex responses, and thus play a major role in the long-lasting spastic reflexes seen after chronic spinal cord injury.

The ability to activate plateaus in normal motoneurons relies on the facilitation of PICs by neuromodulators, including 5-HT (Hounsgaard and Kiehn 1989) and NE (Foehring et al. 1989). Following acute spinal cord transection, the motoneurons can not gain sufficient PICs to sustain plateaus due to the loss of the descending reticulospinal tracts, since the axons containing 5-HT are originated from the raphe nucleus (Maxwell et al. 1996) and the axons containing NE are originated from the locus ceruleus nucleus (Patel et al. 1997). However, it has been found that the motoneurons somehow regain the ability

to produce plateaus over the months following the injury, even in the complete absence of externally applied neuromodulators like 5-HT, and even though the motoneurons are completely isolated from brainstem (Bennett et al. 2001b; Li and Bennett 2003). A central goal of this thesis is to determine what makes these large PICs occur following chronic spinal cord injury. We explore the hypothesis that motoneurons become supersensitive to residual 5-HT in the spinal cord following chronic injury.

Ionic Mechanism Underlying Spasticity and Modulation

The PICs underlying the long lasting reflexes includes two inward currents, a TTX-sensitive sodium current and a low threshold nimodipine-sensitive L-type calcium current. Previously, the PICs responsible for plateaus in motoneurons have been shown to be mediated by L-type calcium channels (Perrier et al. 2002; Simon et al. 2003), possibly through the newly identified low voltage activated Cav1.3 calcium channels (Xu and Lipscombe 2001). This Cav1.3 L-type calcium channel is less sensitive to nimodipine (Hounsgaard and Kiehn 1989) and has lower activation voltage than the conventional L-type calcium channel (Cav1.2) (McCarthy and TanPiengco 1992). According to more recent results, both low-voltage-activated L-type calcium currents and TTX-sensitive persistent sodium currents contribute to the activation of plateaus in both normal motoneurons and motoneurons of chronic spinal animals (Chandler et al. 1994; Li and Bennett 2003; Powers and Binder 2003). The TTX-sensitive persistent sodium currents are activated just sub-threshold to the sodium spike and tend to partly inactivate over a few seconds. In contrast, the L-type calcium current can persist without inactivating for many seconds and contributes the majority of the sustained depolarization seen in

motoneurons. Following chronic spinal cord injury, there are dramatic changes in L-type calcium channels and sodium channels in motoneurons below the level of injury. Through these channels, large persistent calcium currents (Ca PICs) and persistent sodium currents (Na PICs) are activated by brief afferent stimulation, and remarkably, these PICs turn out to be solely responsible for the many second long spasms associated with spasticity (Bennett et al. 2001b; Li et al. 2004a).

After chronic injury, there are still small amounts of endogenous 5-HT (about 2-15% of original) in the spinal cord below the injury (Hains et al. 2002; Newton and Hamill 1988; Shapiro 1997). In normal motoneurons, this low level of 5-HT should not be sufficient to induce substantial sodium or calcium PICs in motoneurons, and indeed even in acute injury PICs are very small (Harvey et al. 2005b). However, it has been shown that the persistent sodium currents (Na PICs) become supersensitive to 5-HT after chronic spinal cord injury, with a Na PIC facilitated by a 5-HT concentration that is only about 3% of the effective concentration in normal motoneurons (30-fold supersensitivity; Harvey et al. 2005b). Thus, the residual small amount of 5-HT in the spinal cord after chronic transection (2 - 12%) should be more than enough to produce large Na PICs (60 - 400% of normal). This idea has been confirmed by showing that blocking the action of endogenous 5-HT (and NE) with 5-HT_{2a}, 5-HT_{2c} and $NE_{\alpha 1}$ receptors antagonist dramatically reduces the spontaneously occurring Na PICs. In combination these three antagonists completely eliminate the Na PIC in chronic spinal rats, demonstrating that residual 5-HT and NE acting on supersensitive receptors play the central role in facilitating Na PICs. Thus, in as far as Na PIC contribute to spasticity (see above; Li et al.

2004a), this finding brings our understanding of spasticity to a new level: residual 5-HT and NE in the spinal cord acting on supersensitive receptors plays a major role in generating spasticity (Harvey et al. 2005c).

It is reasonable to hypothesize that the persistent calcium currents (Ca PICs) also become supersensitive to 5-HT and are also increased by residual endogenous 5-HT after chronic injury. Exploring this hypothesis is the one of the major objectives of this thesis.
However, there are a number of complications to address first, because the Ca PIC is not likely to be mediated by a single current, nor facilitated by the same receptors as the Na PIC. Furthermore, the same receptor may have different effects on these two currents; for example, $GABA_B$ receptor activation (with baclofen) increases the amplitude of the sodium PIC, but decreases the amplitude of the calcium PIC (Li et al. 2004c). Therefore, the sodium PICs need to be separated from the calcium PIC, when the calcium PIC is investigated.

Calcium PIC and Small Conductance Calcium-activated Potassium Channel (SK current)

In order to study the L-type calcium current in isolation, both the sodium PIC and the calcium activated currents need to be blocked. The calcium ion is not simply a charge carrier; it is also capable of activating several calcium-activated channels, including the calcium-activated small conductance potassium channel (SK channel), the calcium activated big conductance potassium channel (BK channel) and the calcium activated

nonselective cationic (I_{CAN}) channel. Therefore, the calcium PIC (Ca PIC) recorded in motoneurons probably is the net L-type calcium current (L-Ca) plus these calcium-activated currents. What is more, when agonists of 5-HT receptors are applied, these calcium-activated currents are likely to increase secondary to the 5-HT induced increases of calcium currents, or even be regulated directly by the agonists, which makes the study of the net calcium PIC even more difficult. Thus, the calcium current through the L-type channels can be investigated only after being isolated from these calcium-activated currents. Among these calcium-activated currents, the interaction between the SK current and the Ca PIC is of particular interest. The reason is that the I_{CAN} current has been shown *not* to play an important role in the plateau potentials in motoneurons (Perrier and Hounsgaard 1999). Also, the BK currents are responsible for the fast afterhyperpolarization (fAHP) and activated primarily by the N-type and P/Q-type calcium channels (Umemiya and Berger 1994), but not L-type calcium currents. What is more, the BK current is unlikely to be important for the plateaus mediated by the sustaining L-type calcium channels due to its relatively transient activation (McLarnon 1995) compared to the slow activation and long time course of the L-type calcium PIC. In comparison, SK channel inactivates slower, is not sensitive to the membrane potential, and the SK conductance increases with higher intracellular calcium concentration (McLarnon 1995). SK channels have been found to be present in most types of neurons and responsible for the medium afterhyperpolarization (mAHP) (McLarnon 1995). Since the SK current is an outward hyperpolarizing current and display relatively long lasting effects (produce mAHPs), they are likely to be activated by the calcium influx through the L-type calcium channels and subsequently counteract these L-type calcium currents.

Previous studies also have shown that the L-type calcium channels are co-located with the SK channels and some types of L-type calcium channels are capable of activating at least some of the SK channels (Bowden et al. 2001). It is certain that the calcium influx during spikes can activate SK currents, which produce the mAHPs (Viana et al. 1993). This outward hyperpolarizing current must counteract the net Ca PIC underlying the sustained firing (Li et al. 2004a). However, during a full spike, both HVA calcium channels and LVA calcium channels are activated. Thus, it is still unclear whether the low threshold L-type calcium current that mediates the Ca PIC (Cav1.3), is capable of activating the SK currents directly. If so, these would counteract the Ca PIC and result in smaller amplitude of the recorded net Ca PIC. Addressing this question is the first topic of this thesis. Previous studies already suggested that the recorded calcium PIC is not a pure calcium current, because the reversal potential of the recorded calcium PIC is very low (-30 to -40mV) (Li and Bennett 2003), which means an outward current (possibly SK current) is activated following the calcium current activation.

Brief Summary of the Thesis Work

The present thesis includes two projects. In the first project, it is demonstrated that the major calcium-activated current that is activated by the low voltage activated L-type calcium current is the SK current. This sets the stage for the second project, where the modulation of the L-type calcium current by 5-HT is studied in isolation, by first blocking SK currents (and Na PICs). Specifically, in the first project, the SK current activated by the L-type (Cav1.3) calcium PIC (termed as SK_L) is studied in motoneurons either from chronic spinal rats or from normal rats. The persistent sodium current is blocked by TTX in all the experiment. By comparing the amplitudes of the calcium PICs before and after the application of apamin (specific SK channel blocker), our results showed that the L-type calcium current (L-Ca) does activate a SK current (SK_L), which subsequently diminishes the recorded calcium PIC (Ca PIC). With apamin to block the SK channel, the recorded calcium PIC is increased and the calcium plateau is enlarged and prolonged as well. The calcium influx source inducing the SK_L current is different from that responsible for the SK current mediating the AHP (SK_{AHP}). N-type and P/Q-type calcium channel blocker conotoxin MVIIC eliminates both fAHP and mAHP, whereas the specific L-type calcium channel blocker nimodipine only blocks the SK_L current without affecting the mAHP (SK_{AHP}). Our results also showed that the amplitude of the SK_L current in the acute spinal rats are not significantly different from that of the chronic spinal rats, though the L-Ca PIC in the chronic spinal rats were significantly bigger. We also quantified the SK currents that mediated the AHPs during firing (termed SK_{AHP}), and ultimately we examined the role of both kinds of SK currents in firing (SK_{AHP} and SK_L).

In the second project, the relatively pure L-type calcium current is isolated by using TTX and apamin to block sodium currents and SK current, respectively. Then, the modulatory effect of 5-HT on the L-type calcium currents and the supersensitivity of these calcium channels to 5-HT is investigated. Our results show that 5-HT has complex effect on motoneurons either from normal rats or chronic spinal rats. The main effects include, the input resistance is increased, the resting membrane potential is depolarized, the calcium PIC is increased, and the activation threshold for the PIC is lowered. Importantly, all these effects are 30-fold supersensitive to 5-HT after chronic injury compared to in normal motoneurons, in that small dose of 5-HT only affect motoneurons of chronic spinal rats, but not in normal rats. Because there is residual 5-HT in the spinal cord following chronic transection (see above and Newton and Hamill, 1988), this residual 5-HT likely acts on the supersensitive 5-HT receptors to help produce the large Ca PIC seen in chronic spinal rats. Ultimately, spasticity therefore results from a developed supersensitivity to monoamines like 5-HT and NE, which remain in the spinal cord at low concentration (2 - 15 % of normal), and act on motoneurons to produced both the large Na PICs (Harvey et al. 2005c) and large Ca PICs (present work) that underlay muscle spasms (Li et al. 2004a).

Animal Model of Spasticity

While spasticity has long been studied, the underlying mechanisms are not well understood, partly due to the lack of appropriate experimental models. Spasticity can be found in humans with partial spinal cord transections. Whereas, in animals, only mild spasticity can be induced by incomplete spinal cord injury (Bennett et al. 1999a; Hultborn and Malmsten 1983). Complete lumbar spinal transections can lead to spasticity in animals if they remain in a healthy state. However, their susceptibility to bladder infections and pressure sores can be a chronic problem (Ashby et al. 1987; Bennett et al. 1999a).

An accessible animal model of spasticity was developed by Ritz in 1992. Ritz's group found that low sacrocaudal transections in cats caused significant spasticity in the axial musculature of the tail vertebrae, without disrupting normal bladder, bowel or locomoter functions (Ritz et al. 1992). In Bennett's lab, a similar model has been developed recently. In this model, a complete spinal cord transection is made at the S2 sacral spinal cord level in adult Sprague Dawley rats. Rats are easier to handle and more resistant to infections compared with cats. By transecting the cord at the S2 level, the locomotion and bowel/bladder function are preserved. Also, the cord below S2 level is mainly responsible for the innervation of the tail muscle, which is easy to test and manipulate. What is more, the muscular structure of the tail muscle is not very different from the structure of the axial muscles of the back in human. Tonic muscle activity usually emerges after two weeks following the injury. After one month's recovery, pronounced spasticity can be

observed in the animals. A brief stimulation (either cutaneous stimulation or muscle stretch) can evoke long lasting reflexes in the tails, which is not seen in normal rats. In summary, the sacral spinal lesions in rats lead to flexor and extensor hypertonus, hyperreflexia, flexor spasms and clonus in the tail muscle, with normal bladder and bowel functions remaining intact. The time course of the development of spasticity in the rat-tail muscle is similar as the development of spasticity in human limbs, and thus suggests a similar mechanism of the spasticity development. Another important advantage of this preparation is, the sacrocaudal spinal cord segment of the rat is very small and thus it is possible to keep this segment alive *in vitro* during the experiments (Bennett et al. 1999a).

Reference

Ashby P, Mailis A, and Hunter J. The evaluation of "spasticity". *Can J Neurol Sci* 14: 497-500, 1987.

Bennett DJ, Gorassini M, Fouad K, Sanelli L, Han Y, and Cheng J. Spasticity in rats with sacral spinal cord injury. *J Neurotrauma* 16: 69-84, 1999.

Bennett DJ, Li Y, and Siu M. Plateau potentials in sacrocaudal motoneurons of chronic spinal rats, recorded in vitro. *J Neurophysiol* 86: 1955-1971, 2001.

Bowden SE, Fletcher S, Loane DJ, and Marrion NV. Somatic colocalization of rat SK1 and D class (Ca(v)1.2) L-type calcium channels in rat CA1 hippocampal pyramidal neurons. *J Neurosci* 21: RC175, 2001.

Chandler SH, Hsaio CF, Inoue T, and Goldberg LJ. Electrophysiological properties of guinea pig trigeminal motoneurons recorded in vitro. *J Neurophysiol* 71: 129-145, 1994.

Foehring RC, Schwindt PC, and Crill WE. Norepinephrine selectively reduces slow Ca2+- and Na+-mediated K+ currents in cat neocortical neurons. *J Neurophysiol* 61: 245-256, 1989.

Gorassini MA, Knash M, Harvey PJ, Bennett DJ, and Yang JF. Role of motoneuron plateau potentials in the generation of involuntary muscle activity after spinal cord injury. *Brain* 127: 2247-2258, 2004.

Hains BC, Everhart AW, Fullwood SD, and Hulsebosch CE. Changes in serotonin, serotonin transporter expression and serotonin denervation supersensitivity: involvement in chronic central pain after spinal hemisection in the rat. *Exp Neurol* 175: 347-362, 2002.

Harvey PJ, Li Y, Li X, and Bennett DJ. Persistent sodium currents and repetitive firing in motoneurons of the sacrocaudal spinal cord of adults. 2005. Submitted to J Neurophysiol.

Harvey PJ, Li Y, Li X, and Bennett DJ. Serotonin facilitates persistent sodium currents in motoneurons, and spinal cord transection leads to a supersensitivity to serotonin. 2005. Submitted to J Neurophysiol.

Harvey PJ, Li Y, Li X, and Bennett DJ. Endogenous monoamines are essential for persistent sodium currents and repetitive firing in rat spinal motoneurons. 2005. In preparation.

Heckman CJ. Alterations in synaptic input to motoneurons during partial spinal cord injury. *Med Sci Sports Exerc* 26: 1480-1490, 1994.

Hounsgaard J and Kiehn O. Serotonin-induced bistability of turtle motoneurones caused by a nifedipine-sensitive calcium plateau potential. *J Physiol* 414: 265-282, 1989.

Hultborn H and Malmsten J. Changes in segmental reflexes following chronic spinal cord hemisection in the cat. I. Increased monosynaptic and polysynaptic ventral root discharges. *Acta Physiol Scand* 119: 405-422, 1983.

Kuhn RA and Macht MB. Some manifestations of reflex activity in spinal man with particular reference to the occurrence of extensor spasm. *Bull Johns Hopkins Hosp* 84: 43-75, 1948.

Lance JW and Burke D. Mechanisms of spasticity. *Arch Phys Med Rehabil* 55: 332-337, 1974.

Levi R, Hultling C, Nash MS, and Seiger A. The Stockholm spinal cord injury study: 1. Medical problems in a regional SCI population. *Paraplegia* 33: 308-315, 1995.

Li Y and Bennett DJ. Persistent sodium and calcium currents cause plateau potentials in motoneurons of chronic spinal rats. *J Neurophysiol* 90: 857-869, 2003.

Li Y, Gorassini MA, and Bennett DJ. Role of persistent sodium and calcium currents in motoneuron firing and spasticity in chronic spinal rats. *J Neurophysiol* 91: 767-783, 2004a.

Li Y, Li X, Harvey PJ, and Bennett DJ. Effects of baclofen on spinal reflexes and persistent inward currents in motoneurons of chronic spinal rats with spasticity. *J Neurophysiol* 92: 2694-2703, 2004b.

Little JW, Micklesen P, Umlauf R, and Britell C. Lower extremity manifestations of spasticity in chronic spinal cord injury. *Am J Phys Med Rehabil* 68: 32-36, 1989.

Maxwell L, Maxwell DJ, Neilson M, and Kerr R. A confocal microscopic survey of serotoninergic axons in the lumbar spinal cord of the rat: co-localization with glutamate decarboxylase and neuropeptides. *Neuroscience* 75: 471-480, 1996.

McCarthy RT and TanPiengco PE. Multiple types of high-threshold calcium channels in rabbit sensory neurons: high-affinity block of neuronal L-type by nimodipine. *J Neurosci* 12: 2225-2234, 1992.

McLarnon JG. Potassium currents in motoneurones. *Prog Neurobiol* 47: 513-531, 1995.
Newton BW and Hamill RW. The morphology and distribution of rat serotoninergic intraspinal neurons: an immunohistochemical study. *Brain Res Bull* 20: 349-360, 1988.

Patel R, Kerr R, and Maxwell DJ. Absence of co-localized glutamic acid decarboxylase and neuropeptides in noradrenergic axons of the rat spinal cord. *Brain Res* 749: 164-169, 1997.

Perrier JF, Alaburda A, and Hounsgaard J. Spinal plasticity mediated by postsynaptic L-type Ca2+ channels. *Brain Res Brain Res Rev* 40: 223-229, 2002.

Perrier JF and Hounsgaard J. Ca(2+)-activated nonselective cationic current (I(CAN)) in turtle motoneurons. *J Neurophysiol* 82: 730-735, 1999.

Powers RK and Binder MD. Persistent sodium and calcium currents in rat hypoglossal motoneurons. *J Neurophysiol* 89: 615-624, 2003.

Ritz LA, Friedman RM, Rhoton EL, Sparkes ML, and Vierck CJ, Jr. Lesions of cat sacrocaudal spinal cord: a minimally disruptive model of injury. *J Neurotrauma* 9: 219-230, 1992.

Shapiro S. Neurotransmission by neurons that use serotonin, noradrenaline, glutamate, glycine, and gamma-aminobutyric acid in the normal and injured spinal cord. *Neurosurgery* 40: 168-176; discussion 177, 1997.

Simon M, Perrier JF, and Hounsgaard J. Subcellular distribution of L-type Ca2+ channels responsible for plateau potentials in motoneurons from the lumbar spinal cord of the turtle. *Eur J Neurosci* 18: 258-266, 2003.

Taylor JS, Friedman RF, Munson JB, and Vierck CJ, Jr. Stretch hyperreflexia of triceps surae muscles in the conscious cat after dorsolateral spinal lesions. *J Neurosci* 17: 5004-5015, 1997.

Thilmann AF, Schwarz M, Topper R, Fellows SJ, and Noth J. Different mechanisms underlie the long-latency stretch reflex response of active human muscle at different joints. *J Physiol* 444: 631-643, 1991.

Umemiya M and Berger AJ. Properties and function of low- and high-voltage-activated Ca2+ channels in hypoglossal motoneurons. *J Neurosci* 14: 5652-5660, 1994.

Viana F, Bayliss DA, and Berger AJ. Multiple potassium conductances and their role in action potential repolarization and repetitive firing behavior of neonatal rat hypoglossal motoneurons. *J Neurophysiol* 69: 2150-2163, 1993.

Xu W and Lipscombe D. Neuronal Ca(V)1.3alpha(1) L-type channels activate at relatively hyperpolarized membrane potentials and are incompletely inhibited by dihydropyridines. *J Neurosci* 21: 5944-5951, 2001.

Young RR. Spasticity: a review. *Neurol* 44: S12-S20, 1994.

Chapter 2: Apamin-sensitive calcium-activated potassium currents (SK) are activated by persistent calcium currents in rat motoneurons

Introduction

Motoneurons have low threshold persistent inward currents (PICs), composed of persistent sodium and calcium currents (Carlin et al. 2000b; Li and Bennett 2003; Powers and Binder 2003; Svirskis and Hounsgaard 1997). These PICs are facilitated by monoamines, such as serotonin (Hounsgaard and Kiehn 1989; Perrier and Hounsgaard 2003) and norepinephrine (NE: Lee and Heckman 1999), which arise mostly, though not exclusively, from the brainstem (Maxwell et al. 1996; Patel et al. 1997). Also, PICs are facilitated by other transmitters such as glutamate and acetlycholine, acting on metabotropic receptors (Svirskis and Hounsgaard 1998). Functionally, PICs are important for bistable behaviour, including production of plateau potentials and self-sustained firing, seen in the normal spinal cord intact animals (Lee and Heckman 1998a, b; Schwindt and Crill 1982) and chronic spinal animals (Bennett et al. 2001b). Furthermore, bistable behaviours have been shown to play a major role in motor unit firing in normal and spinal cord injured humans (Gorassini et al. 1998; Gorassini et al. 2004; Kiehn and Eken 1997). Because of their dependence on facilitation from monoamines, PICs are dramatically reduced, though not eliminated by acute spinal transection, which eliminates brainstem monoamine innervation. However, these PICs return with chronic injury, possibly due to a developed supersensitivity to residual monoamines below the transection (Harvey et al. 2005a,b,c).

The persistent sodium currents (Na PIC) in motoneurons are TTX-sensitive, activate sub-threshold to firing and partly inactivate over a few seconds after activation. The persistent calcium currents (Ca PIC) are nimodipine-sensitive, activated near the firing threshold,

but persist for longer than the Na PIC (seconds to minutes), and thus play the major role in sustained depolarizations (plateaus) and firing (self-sustained firing, Bennett et al. 2001b; Li and Bennett 2003). The calcium PICs responsible for plateaus in motoneurons have been shown to be mediated by L-type calcium channels (Perrier et al. 2002; Simon et al. 2003), likely acting via the newly identified low threshold Cav1.3 calcium channels (Xu and Lipscombe 2001). The calcium PIC can be isolated by blocking the persistent sodium PIC with TTX. Besides acting as a charge carrier, the calcium ion is also capable of activating other channels, such as the calcium activated small conductance potassium channel (SK channel), the calcium activated big conductance potassium channel (BK channel) and the calcium activated nonselective cationic (I_{CAN}) channel. Therefore, the calcium PIC (Ca PIC) recorded in motoneurons is likely the net L-type calcium current (L-Ca) plus the calcium-activated currents. The I_{CAN} current has been shown *not* to play an important role in the plateau potentials in motoneurons (Perrier and Hounsgaard 1999). Also, the BK currents have been found to be responsible for the fast afterhyperpolarization (fAHP) and activated primarily by the N-type and P/Q-type calcium channels (Umemiya and Berger 1994), but is unlikely to play a major role in plateaus mediated by L-type calcium channels due to its relatively transient activation (McLarnon 1995).

SK channels have little voltage-dependence, but great Ca^{2+}-dependent sensitivity. The conductance of SK channels increases with accumulation of intracellular Ca^{2+} and inactivate slowly (McLarnon 1995). The calcium sensitivity of SK channels arises from domains on the C terminal of each of their four subunits, which bind calmodulin as the

Ca^{2+}-sensor (Keen et al. 1999). SK channels have been found to be present in most types of neurons and responsible for the medium duration afterhyperpolarization (mAHP; McLarnon 1995). Previous studies have shown that certain L-type calcium channels are co-located with the SK channels and these SK channels can be activated when the L-type calcium channels are open (Bowden et al. 2001). Since the SK channels hyperpolarize the neurons and display relatively long lasting effects (produce mAHPs), they are likely activated during the Ca PICs, and ultimately should counteract the current produced by the L-type calcium channels. It is certain that the SK currents activated by spikes hyperpolarize the cell, by production of mAHPs, and this SK current must counteract the net Ca PIC that helps sustain firing. However, it is unclear whether the L-type calcium current that mediates the Ca PIC (Cav1.3), also *directly* activates SK currents. If so, these would also reduce the net PIC. Previous studies indicate that the recorded calcium PIC is not a pure calcium current, because the reversal potential of the recorded calcium PIC is very low (-30 to -40mV), suggesting an opposing potassium current is activated following the calcium current activation, and this may be due to the SK current (Li and Bennett 2003). In this paper, the possibility that the L-type calcium current directly activates SK currents (termed SK_L current) is investigated by comparing PICs before and after blocking the SK channels with apamin, which is a highly specific SK channel blocker.

Our study showed that the L-type calcium current (L-Ca) does indeed activate a SK current (termed SK_L), which subsequently diminishes the recorded calcium PIC (Ca PIC). With apamin to block the SK channel, the recorded calcium PIC is increased and the calcium

plateau is enlarged and prolonged as well. For comparison, we also quantified the SK currents that mediated the AHPs during firing (termed SK_{AHP}), and ultimately we examined the role of both kinds of SK currents in firing (SK_{AHP} and SK_L). For this study, we recorded PICs and firing in motoneurons in an *in vitro* preparation (Bennett et al. 1999b) where the sacrocaudal spinal cord was removed either from normal adult rats (acute spinal) or from adult rats after two months spinal cord injury (chronic spinal). These two preparations allowed us to additionally examine whether the SK currents were relatively smaller in chronic compared to acute spinal rats, thus contributing to the large net PICs seen in chronic spinal rats.

Methods

Intracellular recordings were made from motoneurons in sacrocaudal spinal cord of both normal adult rats (female Sprague-Dawley; 3 – 9 months old, n = 8) and spastic adult rats with chronic spinal cord injury (3 – 8 months old, n = 18). The chronic spinal rats were transected at 2 months of age (adult rat) and recordings were made after their affected muscles became spastic (1 – 6 months after injury). See Bennett et al. (1999a) for details of the chronic spinal transection and spasticity assessment. All recordings were made from the whole sacrocaudal spinal cord that was removed from the rat with a S2 sacral transection and maintained *in vitro*. This transection was made in chronic spinal rats just rostral to the chronic spinal injury, so as not to do further damage to the sacrocaudal cord. In contrast, in the normal rats, the spinal cord was necessarily acutely injured in the in vitro preparation (cut at S2), and thus we refer to these motoneurons as from acute spinal rats. Like in other in vitro slice or whole cord preparations, this acute injury produced the characteristic effects of spinal shock, where motoneurons were relatively inexcitable, compared to those of chronic spinal rats or normal intact animals (Bennett et al. 2001a). All experimental procedures were approved by the University of Alberta Health Sciences Animal Policy and Welfare Committee.

In vitro preparation

Details of the experiment procedures have been described in previous publications (Bennett et al. 2001b; Li and Bennett 2003). Briefly, all the rats were anaesthetized with urethane

(0.18 g/100 g; with a maximum dose of 0.45 g), and part of the caudal cord (between the T13 and L6 vertebrae) was exposed and kept wet with modified artificial cerebrospinal fluid (mACSF). The rat was given pure oxygen for 5 minutes before transferred to a dissection chamber containing mACSF. All spinal roots were removed, except the S4 and Ca1 ventral roots. The cord was secured by gluing the dorsal surface of the cord onto a small piece of nappy paper. After a 1.5 hours of incubation in the dissection chamber at room temperature (20-21° C), the cord was transferred to a recording chamber containing normal artificial CSF (nACSF) maintained at 23-25° C and with a flow rate > 5 mL/min. The cord was fixed onto the bottom of the recording chamber with the ventral side up by pinning the nappy paper to the Sylgard base of the chamber. A one hour long exposure in nACSF was given to wash out the residual anaesthetic and kynurenic acid, and then the nACSF was recycled as follows. The nACSF was oxygenated in a 200-mL source bottle, and then run through the recording chamber. This nACSF running out of the recording chamber was collected, filtered and returned to the source bottle with a pump. Because of the large volume (200 mL) of the source bottle and the small volume of the cord (< 0.05 mL), the accumulation of any possible metabolic byproducts would be negligible.

Intracellular recording

Intracellular recording methods were as described in Li and Bennett (2003) and were briefly summarized here. Sharp intracellular electrodes were made from thick-walled glass capillary tubes (1.5mm O.D.; Warner GC 150F-10) using a Sutter P-87 micropipette puller and filled with a mixture of 1M K-acetate and 1M KCl. Electrodes were bevelled down

from an initial resistance of 40-80 MΩ to 25-30 MΩ using a rotary beveller (Sutter BV-10). A stepper-motor micromanipulator (660, Kopf) was used to advance the electrodes through the tissue and into cells. Intracellular recordings from motoneurons were made with an Axoclamp 2b intracellular amplifier (Axon Instruments, Burlingame, CA) running in discontinuous current clamp (DCC, switching rate 5-8 kHz, output bandwidth 3.0 kHz) or discontinuous single-electrode voltage clamp (SEVC; gain 0.8 to 2.5 nA/mV) modes. The S4 and Ca1 ventral roots were wrapped around Ag/AgCl electrodes above the recording chamber and sealed with high-vacuum grease (Dow Corning Corp.), which allowed for antidromic stimulation and thus used to identify motoneurons. Motoneurons with a resting potential below -60 mV and antidromic spike overshoot over 0mV were considered healthy and used for recording. We also recorded from motoneurons after TTX was applied to block all the sodium channels, though we could not directly identify these as motoneurons by antidromic stimulation, because of the block of the antidromic spike by TTX. However, we found that these neurons could be reliably be identified as healthy motoneurons by their characteristic location (depth in motor nucleus), resting potential (Vm; -75 to - 60 mV), input resistance (Rm) and capacitance (Cm), the latter measured from the response to a 0.4 nA hyperpolarizing current step. The capacitance was estimated from the time constant, τ, of an exponential fit to the response, which equals the product Rm * Cm (see details in Results).

Drugs and solutions

Two kinds of artificial cerebrospinal fluid (ACSF) were used in these experiments; a modified ACSF (mACSF) in the dissection chamber prior to recording and a normal ACSF (nACSF) in the recording chamber. The mACSF was composed of (in mM) 118 NaCl, 24 $NaHCO_3$, 1.5 $CaCl_2$, 3 KCl, 5 $MgCl_2$, 1.4 NaH_2PO_4, 1.3 $MgSO_4$, 25 D-glucose and 1 kynurenic acid. Normal ACSF was composed of (in mM) 122 NaCl, 24 $NaHCO_3$, 2.5 $CaCl_2$, 3 KCl, 1 $MgCl_2$ and 12 D-glucose. Both types of ACSF were saturated with 95% O_2-5% CO_2 and maintained at pH 7.4. Additional drugs were added as required, including 2 μM tetrodotoxin (TTX; Alamone Labs, Israel), 0.15 μM apamin (Alamone Labs, Israel), 15 μM nimodipine (Sigma) and 5 μM conotoxin G-VII-C (Sigma). The spinal cords were briefly exposed to nACSF solution containing 0.04% pronase E (Helixx Technologies) for 10 seconds prior to recording to weaken the pia of the spinal cords and allowed for easier penetration (Buschges 1994).

Persistent inward currents in current and voltage clamp recording

Slow triangular current ramps (0.4 nA/s) were applied to the motoneurons to induce firing and associated AHPs, and measure basic cell properties. The input resistance was measured during the ramp over a 5-mV range near rest and subthreshold to PIC onset. The plateau potential was seen as a subthreshold acceleration in membrane potential prior to the firing threshold and a long after-depolarization following cessation of firing. Instantaneous firing frequency (F) was computed from the current ramp recordings, using Clampfit 9.0 software.

Slow triangular voltage ramps (3.5 mV/s) were applied to measure the PICs in voltage clamp. During the upward portion of the ramp, the current initially increased linearly with voltage in response to the passive leak conductance. A linear relation was fit in this region (10 mV below the PIC onset) and extrapolated to the whole range of the ramp. At more depolarized potential and the PIC threshold was reached, there was a downward deviation from the extrapolated leak current. The amplitude of the PIC was measured as the peak amplitude of this downward deviation. Large PICs usually caused a negative slope in the current response. Smaller PICs only caused a downward deflection in the current response (flattening of I-V slope) without a negative-slope region. The onset voltage for the PIC (V_{on}) was defined as the voltage at which the I-V slope first reached zero (Li and Bennett 2003). V_{on} is not possible to be determined in cells without a negative-slope region. The current value corresponding to V_{on} was defined as I_{on}. The width of the PIC (V_w) was defined as the span between V_{on} and the voltage at which the current reached I_{on} for the second time on the upward section during the ramp (defined as V_{jump}), that is, $V_w = V_{jump} - V_{on}$. Previously, it has been shown that the width of the PIC corresponds to the amplitude of the plateau potential that produced by the PIC (Li and Bennett 2003). The spike voltage threshold (V_{th}), was averaged from five consecutive spikes starting with the second spike on the up ramp, and was taken as the voltage at which the rate of the membrane potential change (dV/dt) higher than 10V/s (Li et al. 2004a).

Analysis of AHP, and its conductance and voltage dependence

The AHP was initially quantified when the membrane potential was held subthreshold to repetitive firing, by evoking spikes with antidromic stimulation of the ventral roots. The maximum AHP amplitude was taken as the amplitude of the mAHP, the duration was quantified as the duration of the mAHP at half its amplitude (half amplitude).

The dependence of the AHP amplitude on potential was measured by systematically varying the potential prior to the antidromic stimulation with a bias current. As described in the results, the AHPs measured in this way had a linear voltage dependence, and we thus fit a linear regression the AHP versus potential relation and made the following calculations to quantify this voltage dependence. The conductance of the SK channels is known *not* to have a voltage-dependence itself (Lancaster et al. 1991), and so it can be thought of a simple fixed conductance (G_{AHP}). Therefore, the SK current (I_{SK}) underlying the AHP can be approximately modeled as the product of this SK conductance and the difference between the potential (V) and the reversal potential for potassium (E_K), thus explaining the linear dependence of the AHP on potential. That is, $I_{SK} = G_{AHP}(V - E_K)$. This SK current ($I_{SK}$) ultimately acts through the leak conductances G_L and the SK conductance itself to produce the mAHP:

$$mAHP = G_{AHP}(V - E_K)/(G_{AHP} + G_L) \quad \text{.....(1)}$$

From this equation (1), the potential V at which the mAHP is zero corresponds to the reversal potential for potassium, E_K, and this was computed from the regression line fit through the AHP versus potential relation. The slope of the AHP versus potential relation (S_{AHP}) was measured for each cell from the regression fit. This slope can be seen from equation (1) to be equivalent to $S_{AHP} = G_{AHP}/(G_{AHP} + G_L)$, and rearranging this relation

gives an estimation of the AHP conductance: $G_{AHP} = G_L S_{AHP}/(1 - S_{AHP})$, which was also computed for each cell.

Data analysis

Data were analyzed in Clampfit 8.0 (Axon Instruments, USA), and figures were made in Sigmaplot (Jandel Scientific, USA). Data are shown as mean ± standard deviation. A Student's t-test was used to test for statistical differences, with a significance level of $P < 0.05$.

RESULTS

Motoneuron properties and excitability

Intracellular recordings were made from 18 motoneurons from chronic spinal rats and 8 motoneurons from acute spinal rats, while the whole sacrocaudal spinal cord was maintained in vitro. In the latter motoneurons, the sacrocaudal cord was obtained from normal adult rats, but we referred to these as acute spinal rats, because the cord was necessarily cut to remove it from the animal for in vitro recording. The effects of apamin on these motoneurons were studied as described below, and were found to be qualitatively similar in acute and chronic spinal rats. However, we focused on chronic spinal rats because their motoneurons have previously been described to have large robust PICs (Li and Bennett 2003) with associated plateau properties (self-sustained firing) similar to in intact animals and humans (Gorassini et al. 2004; Heckman and Lee 1999b), presumably because they have somehow adapted to the injury (Harvey et al. 2005a, b). Furthermore, motoneurons of these adult chronic spinal rats were much easier to penetrate and stably record from, than motoneurons of acute spinal rats, perhaps because the dense white matter and connective tissue of these fully adult rats had thinned following chronic injury (Bennett et al. 1999b).

The basic properties (Rm, Cm, and Vm) of motoneurons in chronic and acute spinal rats are summarized in Table 2-1. While most neurons were directly identified by antidromic stimulation of the ventral roots (see Methods), a few of the neurons included in this study

(n = 5) were penetrated after all spikes were blocked with TTX, and thus definitive identification with antidromic stimulation was impossible. However, these neurons were recorded from the motor nucleus, and had the characteristic input resistance (Rm= 8.4±1.1MΩ), capacitance (Cm= 850±20 pF), resting potential (Vm < -60 mV) and Ca PICs (2.1±0.7nA) of motoneurons (compare to Table 2-1), and thus we also refer to these as motoneurons. Also, the time constant (RmCm = τ) in these neurons recorded in TTX was typical of that seen in antidromically identified motoneurons (6.4±3.9ms), and in general we found that looking for cells with such long time constants (rise time during current step) was an effective way to initially find putative motoneurons, whether or not TXX was applied.

	Vm(mV)	Rm (MΩ)	Time constant τ (ms)	Capacitance (pF)
Acute (n=8)	-69.9 ± 6.0	9.1 ± 4.1	4.5 ± 2.3	770 ± 20
Chronic (n=18)	-69.8 ± 8.1	8.2 ± 2.9	6.1 ± 3.1	1100 ± 40

Table 2-1 Basic properties of motoneurons

The mAHP is mediated by an apamin-sensitive SK current

In normal ACSF, the sodium spike that was evoked by either antidromic stimulation of the ventral roots (n=12, see Fig 2-1A) or a current injection (n=15, see Fig 2-2A&B) was always followed by a post spike afterhyperpolarization (AHP). This AHP had a classic

combination of a small fast AHP (fAHP) followed by a pronounced medium duration AHP (mAHP) (Viana et al. 1993). At the end of a series of spikes (burst) there was a final AHP (Fig 2-2A), but this was not longer than a typical mAHP, and thus there was not the very slow AHP seen in other neurons (no sAHP; Lasser-Ross et al. 1997).

When the potent and selective SK channel blocker apamin (0.15 μM) was applied, the mAHP was completely blocked, and there only remained the fAHP, which was insensitive to apamin (Fig 2-1B,C; n = 9/9 motoneurons in chronic spinal rats and n = 5/5 in acute spinal rats). This mAHP block was seen by comparing the spike evoked by antidromic stimulation from potentials subthreshold to repetitive firing, as in Fig 2-1C, or by comparing the first spikes when repetitive firing was evoked by a ramp current injection, as in Fig 2-2 C, E, Thus, an apamin-sensitive calcium-activated potassium current (SK current) mediates the entire mAHP in these motoneurons.

The mAHP limits the firing rate

During repetitive firing in motoneurons, the mAHP plays a central role in limiting the firing rate, roughly maintaining interspike intervals longer than the time to peak of the mAHP (36.5 ± 6.5ms; Kernell 1965; Li et al. 2004a). Such firing is seen in Fig 2-2A, where firing only reached 10 Hz during a slowly increasing current injection, and then decreased relatively linearly as the current was decreased. In contrast, when the mAHP was blocked with apamin as shown in Fig 2-2B, the firing rate at recruitment jumped extremely rapidly (in an all-or-nothing manner) to a very high rate not normally obtained

in these motoneurons (100 Hz in Fig 2-2B, note scale difference), and 10-times higher than the rate for the same current ramp prior to apamin. Basically, in apamin there was only the fAHP to limit the firing rate and this was < 10 ms long, allowing 100 Hz firing immediately. Following recruitment, there was marked spike-frequency adaptation (decrease in rate from 100 Hz to zero), likely due to the inactivation of the sodium channel (spike height reduced). However, the firing did not fail completely and continued at a slower rate after the initial steep spike-frequency adaptation.

The mAHP limits the Ca PIC activation

When there are persistent calcium and sodium currents (Ca and Na PICs) present, the firing is augmented and prolonged by these extra intrinsic currents in the motoneuron (e.g. Li et al. 2004a). This is seen in Fig 2-2A, where the firing is maintained at currents well below the current to recruit the cell (self-sustained firing, hysteresis), mainly due to the activation of Ca and Na PICs (see details in Li et al. 2004a). It has previously been argued that the AHP provides a major hyperpolarizing current that prevents full all-or-nothing activation of the Ca PIC (Li et al. 2004a). Thus, we used an apamin block of the AHP to directly test this idea. Just after termination of firing on a decreasing current ramp, and even just before, there was a clear plateau potential, seen as a deviation from the extrapolated subthreshold changes in potential with current (thin line, plateau ~ 15 mV in Fig 2-2B), and this was much larger than the small after-potential (plateau; at upward arrow in Fig 2-2A) seen without apamin (Fig 2-2A). This plateau was due to a Ca PIC, because it persisted when the Na PIC and spikes were blocked in TTX (see Fig

2-7 described below). The Ca PIC/plateau (and Na PIC) was initiated just prior to the recruitment with and without apamin (at *'s in Fig 2-2A,B), and thus played a central role in recruitment (Li et al. 2004a). However, in apamin, this Ca PIC was able to more fully activate during firing because of the lack of hyperpolarization from the mAHPs, and ultimately caused the all-or-nothing jump in firing rate at recruitment and a very large after-potential.

Motoneurons without a large enough Ca PIC to produce a plateau (i.e. in acute spinal rats, 5/5; and in 1/9 chronic spinal rats) fired roughly in proportion to the injected current prior to apamin, with no self-sustained firing (not shown, but see Bennett et al. 2001 and Li et al. 2004). With the application of apamin, even these cells reached extremely high rates (near 100 Hz) with standard size current ramps that normally only produced 10 – 15 Hz firing without apamin, but this firing only reached a peak (100 Hz) at the peak of the current injection, rather than at the onset of firing because there was not a large Ca PIC at the onset of firing (not shown). Thus, even without the Ca PIC, sufficient current injection alone caused apamin treated motoneurons to fire at very high unphysiological rates, because they did not have a mAHP to limit the firing rate.

Very slow firing does not require the mAHP

In normal ACSF, there was often very slow firing near the threshold for de-recruitment (in cells with large healthy Na PIC; Li et al. 2004; Harvey et al. 2005a). This very slow firing was at intervals that well exceeded the mAHP duration (see last few spike intervals

in Fig 2-2D), and has previously been shown to result from a near-threshold slow oscillation of the Na PIC, where the Na PIC causes a characteristic slow ramp (at double arrow heads) and then an acceleration in the membrane potential that triggers a spike (at *; referred to as ramp&acceleration profile; this profile is blocked by a low dose of TTX that blocks the Na PIC but not the spike; see details in Li et al. 2004). Following each spike the AHP deactivates the Na PIC and then the Na PIC-dependent ramp&acceleration profile occurs again and triggers another spike (see two interspike intervals shown in Fig 2-2D), and the Na PIC continues to oscillate in this slow manner producing the slow firing, with one spike per oscillation cycle.

Following the block of the mAHP with apamin, this slow firing persisted, again with a characteristic Na PIC-dependent ramp&acceleration profile (at double arrows and * in Fig 2-2F) producing long interspike intervals. This Na PIC-dependent ramp&acceleration profile followed immediately after the fAHP (Fig 2-2F), whereas without apamin this ramp&acceleration profile occurred later, after the mAHP (above dashed line in Fig 2-2D). Thus, apparently the hyperpolarization from the fAHP alone is sufficient to deactivate the Na PIC and following this the Na PIC activates again in the characteristic ramp&acceleration profile (see two interspike interval at left of Fig 2-2F).

It should be emphasized that subthreshold to the Na PIC activation (near -60mV, which is also subthreshold to repetitive firing) this ramp&acceleration profile *never* occurred following a spike evoked by an antidromic ventral root stimulation in apamin (Fig 2-1B),

consistent with it being mediated by the Na PIC. Instead, the membrane potential came back to rest within 20 ms following the spike (mAHP completely blocked by apamin).

The AHP depends on N-, P/Q-type and not L-type calcium currents

When all the calcium currents were blocked with cadmium (400uM), the mAHP was completely blocked (n = 4), consistent with the above conclusion that the mAHP is mediated by a *calcium*-activated potassium current (SK current). A selective block of the high voltage-activated N-, and P/Q-type calcium channels with ω-conotoxin MVIIC (5μM, n = 5) mimicked the effects of cadmium, again completely eliminating the mAHP (fAHP also eliminated, Fig 2-3B). This conotoxin had no effect on the low voltage-activated Ca PIC (see Li and Bennett, 2003). In contrast, a block of the L-type calcium channels with nimodipine had no effect on the AHP (mAHP or fAHP, Fig 2-3C), whereas nimodipine completely blocked the Ca PIC (which is thought to be Cav1.3 L-type calcium channel mediated; see Fig 2-5 described below and Li and Bennett, 2004). Thus, the mAHP in motoneurons is produced by an apamin-sensitive SK current that is activated by calcium that flows through N- and P/Q-type HVA channels during the spike. Further, the L-type calcium channels do not appear to play a major role in the AHP, in contrast to their principle role in producing the low voltage activated Ca PIC (see details below).

The AHP is strongly voltage-dependent, but does not change with chronic injury

In order to compare the AHP across cells and between acute and chronic spinal rats, we found it necessary to first quantify the strong voltage-dependence of the mAHP, which occurred because the mAHP current is a pure potassium current close to its reversal potential (E_K; see Methods). That is, when the mAHP was measured from antidromically evoked spikes while the membrane potential was systematically varied with a bias current (e.g. –70 mV shown in inset of Fig 2-4A), then the mAHP amplitude varied linearly with the membrane potential (subthreshold to repetitive firing, Fig 2-4A). As expected, apamin blocked the mAHP at all potentials (triangles in Fig 2-4A), and thus the mAHP resulted from just an SK potassium current, regardless of the potential. At the fixed potential of –70 mV (near rest), the mAHP was not significantly different in acute and chronic spinal rats. The reversal potential for the mAHP, and thus also E_K, was on average –80mV and –82mV in chronic and acute spinal rats (computed where regression lines crossed 0 mV), and there was no significant difference between these two groups. Because the potassium concentration gradient was not likely to change from cell to cell, the variability in E_K was probably just a result of error in recording absolute potential (e.g. tip potential drift etc). Thus, to compensate for this error in Fig 2-4C we corrected the potentials in all cells so that they had a common E_K, equal to the overall mean E_K (-81mV). After this correction, there was a very close overlap of the AHP-*vs*-potential relations, suggesting that at a given potential, the AHP was very similar in all cells. In particular the mAHP at the corrected –70mV potential was again not significantly different in acute and chronic spinal rats. Of course, the reversal potential for mAHP only represents the reversal

potential as seen at the soma, and if the mAHP currents are distal to the soma it might be expected to be more hyperpolarized. However, because mean reversal potential is only -81 mV and the mAHP varies remarkably linearly with potential, it is likely that the mAHP currents are from channels near the soma.

The slope of the mAHP *vs* potential relation (S_{AHP}, in Fig 2-4B) was also not significantly different in acute and chronic spinal rats. Furthermore, as detailed in the Methods, this S_{AHP} slope can be used to compute the effective conductance of the mAHP (G_{AHP}), and this is summarized in Table 2-2 (0.1 – 0.3 uS), and is also not significantly different in acute and chronic spinal rats. The current underlying the mAHP (I_{SK}) can be directly measured following a simulated spike (2 ms step to > 0 mV) in voltage clamp, as shown in Fig 2-4D. From this current the AHP conductance can be more directly computed by dividing by the driving potential: $G_{AHP} = I_{SK}/(V - E_K)$, and for the example in Fig 2-4D this corresponds to 3 nA/(-50+80 mV) = 0.1 uS, which is similar to the G_K values computed from S_{AHP} (Table 2-2). Finally, the mAHP duration (time to peak mAHP) was on average not significantly different in chronic spinal rats (85.2±16.1ms) compared to in acute spinal rats (77.3±15.9ms).

	mAHP amplitude (mV)	mAHP half duration (ms)	mAHP slope (S_{AHP})	Leak conductance	AHP reversal potential (mV)	mAHP conductance (G_{AHP})
Acute (n=8)	5.22 ± 0.73	77.3 ± 15.8	0.44 ± 0.06	0.24 ± 0.10	80.0 ± 4.7	0.19 ± 0.11
Chronic (n=17)	5.71± 1.47	85.2 ± 16.1	0.48 ± 0.12	0.22 ± 0.04	83.1 ± 2.9	0.23 ± 0.13

Table 2-2 mAHP properties and leak conductances of motoneurons

In summary, the AHP varies dramatically with potential, due to the close proximity of the resting potential to the reversal potential for potassium. Despite this, at a given potential the AHP is not significantly different in amplitude, duration or conductance in acute and chronic spinal rats, and for that matter very similar across all cells.

L-type calcium current of the Ca PIC activates an SK current

When the membrane potential was slowly increased under voltage-clamp conditions, a persistent inward current (PIC) was activated, and seen as a downward deviation from the extrapolated subthreshold linear leak current (thin line), and this usually produced an outright negative slope region in the current-voltage (I-V) relation (NSR; Fig 2-5C). The voltage clamp had adequate gain to usually stop spikes from occurring above the firing threshold (near -51 mV, though one unblocked spike occurred at * in Fig 2-5A; blanked out), and thus AHP currents did not generally contaminate the PIC measurements prior to TTX application, and spikes were blocked after TTX application.

Part of this PIC was blocked rapidly by TTX (about half), and this has previously been attributed to a persistent sodium current in these motoneurons (Na PIC; Fig 2-5A; Li and Bennett, 2003). The remaining current in TTX was blocked by nimodipine (15 μM; leaving only a linear leak current-voltage relation below – 40 mV) and thus was mediated by an L-type calcium channel dependent persistent calcium current (Ca PIC; Fig 2-5C; see details in Li and Bennett, 2003). This Ca PIC is the focus of the remainder of the results section. In chronic spinal rats the Ca PIC was activated with an average onset

threshold of –58.6 mV, and reached a peak of 2.2±1.2 nA at -54 mV. With decreasing current ramps (Fig 2-7, described later) the Ca PIC was deactivated at a significantly lower voltage than its onset voltage (V_{off}; 12.5±3.3 mV lower). Acute spinal rats had similar, but much smaller Ca PICs described later (Fig 2-9).

When apamin was applied to block the outward SK currents (in the presence of TTX) there was a significantly larger persistent inward current measured during voltage ramps (Fig 2-5B, D), which we refer to as the L-Ca current, to distinguish it from the Ca PIC (prior to apamin) and to indicate that it is produced by L-type calcium channels. The apamin-sensitive current (Ca PIC minus L-Ca current) we refer to as the SK_L current (Fig 2-5B). This SK_L current must have been activated by the L-Ca current because it was always activated just after the onset of the L-Ca current (Figs 2-5B and D). Furthermore, the SK_L current must be nimodipine-sensitive, because both the L-Ca current (in apamin; Fig 2-5D) and the Ca PIC (pre apamin; Fig 2-5C) were blocked by nimodipine, and their difference is the SK_L current. The SK_L current at the initial peak of the L- Ca current (at arrow in Fig 2-5B) was on average 0.59 ± 0.4 nA, which was 26% of the L-Ca current. This initial SK_L current was significantly smaller in size and estimated conductance (0.019 +- 0.014 μS; current / $[V-E_K]$) than the SK current underlying the AHP. However, as described below, the SK_L current increased substantially as the voltage ramp continued to increase (at wall). What is more, the width of the valley formed by the PIC in the I-V relation (as defined in Fig 2-7A&B and methods, V_{jump}-V_{on}) was significantly increased, from 11.9 ± 2.7mV (Ca PIC) in control conditions to 13.9 ± 4.1mV (L-Ca PIC) in apamin, consistent with the larger plateau formed in apamin (see below and Methods).

Neither the resting membrane potential nor the leak conductance (1/ Rm) were significantly affected by apamin, and thus there was not a resting calcium current (different from L-Ca) that activated an SK current.

The SK current produced a steep increase in conductance (wall)

In normal ACSF, during the increasing voltage ramp the slope of the I-V response relation was always much steeper after the full activation of the Ca PIC (termed slope conductance S2, and measured after peak of Ca PIC at V_{jump}; dashed vertical line in Fig 2-5D) compared to before the Ca PIC activation (S1, leak conductance; Fig 2-5, A-D). The greater slope conductance after Ca PIC activation (S2/S1 = 2.5±1.2) resulted from: (1) the increased conductance arising from the L-Ca current (Li et al. 2004a), and (2) the activation of SK_L currents. That is, application of apamin significantly lowered the S2 slope relative to the S1 slope (S2/S1 ratio = 1.6±0.5). Characteristically, in apamin the current during the voltage ramp increased linearly after the initial onset of the L-Ca (after NSR), consistent with the onset of a steady L-Ca current that simply increased the overall conductance (by 20 % of leak conductance in Fig 2-6B). In contrast, prior to apamin, the current during the voltage ramp increased much more steeply after the initial onset of the Ca PIC (after NSR), with a non-linear parabolic shape induced by the SK current, as though intracellular calcium was accumulating. Thus, the steep apamin-sensitive S2 slope provides a distinctive feature of the I-V relation that indicates the presence and size of the SK_L current. By subtracting the S2/S1 conductance ratios before and after apamin, we get

the ratio of the SK_L conductance to the leak conductance (S1), which was 0.85 ± 0.8, indicting that the SK_L current produced a conductance similar in size to the leak conductance (and AHP conductance). This steep apamin-sensitive S2 slope conductance was eliminated by nimodipine (Fig 2-5C), as well as apamin (Fig 2-5D), further supporting the idea that the L-Ca current activates an SK current (SK_L).

The detailed changes in the SK current during the voltage ramp can be seen in Fig 2-6D, estimated by subtracting the measured currents before and after apamin (Fig 2-6C). As the membrane potential was depolarized to near – 40 mV, this outward SK_L current always became very large and eventually exceeded the inward L-Ca current; so the net current exceeded the leak current estimate (current above thin leak line in Fig 2-6A). At this point (near - 40 mV) the SK_L current (1.68 ± 0.58nA) was significantly larger than the SK_L current at the initial peak of the PIC (near –50 mV; 0.59 ± 0.4nA; described above), and comparable in size (> 1 nA) to the current produced by the AHP (SK_{AHP}). This large increase in SK current near – 40 mV was generally so pronounced that our intracellular electrodes could not depolarize the cell much past – 40 mV (electrode current limited to < 6 – 12 nA), and thus we also referred to this steep S2 slope region as the *wall* (Fig 2-6C). Once the wall was eliminated by apamin (S2 reduced), we could usually depolarize the cells above – 40 mV (Fig 2-6C; gray section). In current clamp the effect of the wall was manifested as a flat (shallow) region, where the membrane potential could not be easily depolarized by current injection (top of plateau described later in Fig 2-7).

Calcium spikes and post calcium spike afterhyperpolarizations (CaAHPs)

When the Ca PIC was large enough to produce a negative-slope region in the I-V relation (NSR; in voltage-clamp), there was always a plateau potential seen in current clamp during a ramp current injection, induced by the instability of this NSR (Li and Bennett 2003; Schwindt and Crill 1982). This plateau had a characteristic sharp overshoot at its onset (Fig 2-7, D&G), which can be considered as a calcium spike riding on top of the plateau (L-Ca mediated spike). Following this calcium spike there was always a post calcium spike afterhyperpolarization (CaAHP), which tended to reduce plateau. This CaAHP was blocked by apamin and thus was mediated by an SK_L current. In some cells this CaAHP was sustained during the plateau and served to thus reduce the plateau amplitude (Fig 2-7, G-I). However, in other cells the CaAHP reached a peak hyperpolarization in about 200 – 300 ms, and was then turned off, presumably because the CaAHP reduced the L-Ca current underlying the plateau/spike. Following this there was a second calcium spike as the L-Ca current reactivated, followed by a second CaAHP. This oscillation of the L-Ca and the SK current continued for a few cycles until a steady state activation of the L-Ca and the SK currents was reached. This oscillation was always blocked by apamin, confirming the role of the SK_L currents (Figure 2-7, D-F). Further, in apamin the steady-state depolarization was less than without apamin, showing that the SK_L current also produced a steady hyperpolarization throughout the plateau, reducing its size. Interestingly, during voltage ramps a similar oscillation was also seen at the onset of the Ca PIC (Fig 2-7A), even though this current was measured under voltage clamp, which should at least clamp the potential near the soma, avoiding

local oscillations of channels. These oscillations were blocked by apamin (Fig 2-7B), and thus again were mediated by SK_L currents. Likely, these oscillations resulted from calcium spikes interacting with CaAHPs, as described above under current clamp, but occurring in the distal unclamped dendrites. Indeed, all cells that had these Ca PIC oscillations under voltage clamp conditions also had calcium spikes and CaAHP oscillations under current clamp conditions (e.g. Fig 2-7 A and D is from same cell). This provides indirect, but intriguing, evidence that the SK_L currents are of dendritic origin, like the L-Ca currents, and perhaps unlike the SK_{AHP} currents.

Time course of SK_L current

To examine the time course of the SK_L currents we employed a series of long voltage steps. Subthreshold to the Ca PIC, these steps produced a current response proportional to the leak current (trace 1 and 2 in Fig 2-8B, E and left of Fig 2-8F). For larger steps above threshold the Ca PIC was activated and reduced the current below the expected leak current (traces 3 and 4 in Fig 2-8B, E and right of Fig 2-8F). As previously reported, with steps just above threshold for the Ca PIC (trace 3), the Ca PIC activated with a substantial delay, of 1 sec or more (Li and Bennett 2003). Usually a few of the characteristic SK_L-mediated oscillations (apamin-sensitive) occurred during this slow Ca PIC activation (like on current ramps; Fig 2-7B). With larger voltage steps, Ca PIC activated more rapidly, starting at the onset of the step and reaching 90 % of its maximum within 45 ± 7 ms (n = 4), though steady-state activation was not reached for about 1 sec (see below). In contrast, the first sign of the SK_L current onset, seen as small SK-mediated oscillation

(first inflection), did not occur until 170 ± 19 ms. Thus, the SK current onset was delayed by about 100 ms, relative to the underlying L-Ca current that activated it. Thus, the L-Ca activation of the SK currents was slower than the sodium spike-mediated activation of the SK currents (AHP onset in < 10 ms), suggesting differences in spatial location.

Application of apamin increased the overall PIC measured with voltage-steps, as expected from the voltage-ramp results, and consistent with a block of the outward SK currents, leaving only the underlying L-Ca current (Fig 2-8E). The L-Ca, like the Ca PIC, was slow to activate with small voltage steps near threshold, but did not have oscillations during activation (Fig 2-8E; trace 3). With larger steps the L-Ca started its activation sooner, just like the Ca PIC. The net SK current in response to a large step is shown in Fig 2-8C, computed by subtraction before and after apamin. Interestingly, following its onset the SK current was gradually reduced over a few seconds, even though the L-Ca was not reduced (L-Ca computed by leak subtraction, Fig 2-8C). This slow reduction of the SK current with time caused the net Ca PIC (prior to apamin) to reach a steady-state maximum inward current significantly later than the L-Ca current (95 % activation occurred at an average time of 2.3 ± 0.9 seconds for the Ca PIC and 1.1 ± 0.7 seconds for the L-Ca).

Following termination of the voltage steps, the Ca PIC always took about 0.5 second to turn off, producing a characteristic tail current, with a mean duration 323 ± 372 ms prior to apamin (50% down). Associated with this tail current, there was a residual SK current that also decayed off slowly (Fig 2-8C). Block of the SK current with apamin ultimately

led to a significantly longer tail current (783 ± 965ms). Thus, the outward SK current acted to speed the deactivation of the inward L-Ca current.

SK_L currents in acute spinal rats

Motoneurons of acute spinal rats had small but significant Ca PICs, as previously described (Harvey et al. 2005a). These Ca PICs, were not usually large enough to produce a negative slope region (NSR) in the current response to a voltage ramp, and instead only induced a negative deflection in current relative to the extrapolated leak current (PIC indicated by arrow in Fig 2-9A). Because of the lack of NSR, there were also not plateaus seen with current injection in these motoneurons (not shown). Apamin increased these PICs (arrow larger in Fig 2-9B), indicating that there was an apamin-sensitive SK_L current (Fig 2-9D), like in chronic spinal rats. Also, apamin tended to decrease the S2 slope (Fig 2-9B), like in chronic spinal rats, indicating a substantial SK_L conductance.

As expected, the L-Ca current measured in apamin was significantly smaller in acute compared to chronic spinal rats (Fig 2-10A). However, the SK current itself was unexpectedly *not* significantly smaller in acute compared to chronic spinal rats (though its mean was 30% smaller). Also, the SK-induced slope conductance (S2) was not significantly different in acute and chronic spinal rats. Taken together, these results suggest that for a given amount to calcium current (L-Ca) the resulting SK_L current activation was greater in acute spinal rats. Indeed, the ratio of the SK_L current to the L-Ca

current was significantly greater in acute spinal rats by about 40%, compared to in chronic spinal rats (Fig 2-10B).

Barium also blocks apamin-sensitive SK current

To further examine the calcium-activated currents, including SK currents as well as others, we substituted barium (Ba) for calcium (Ca) as the charge carrier through the calcium channels (n=5). This effectively blocks all calcium-activated currents (including the SK current), because barium is much less effective than calcium in activating these currents (Enomoto et al. 1991). As shown in Fig 2-11B, this barium substitution, always led to an increase in the PIC (labeled L-Ba), compared to in normal calcium containing ASCF (Ca PIC), very much like we saw with apamin. Unfortunately, because the barium current through calcium channels is generally known to be larger than the calcium current through the same channels (Hille, 2001), part of this increase in the PIC may have been due to this differing current carrying capability of barium. However, the shape of the I-V relation in barium was remarkably like that in apamin (Fig 2-6B), suggesting that the barium substitution caused a block of SK currents. Indeed, this was the case, because applying apamin while in barium had no significant effect on the PIC (L-Ba is apamin resistant). In barium alone, like in apamin, the S2 slope after the PIC activation was very shallow, and close to the leak conductance (S1), again consistent with barium blocking the SK current that produced the characteristic very steep S2 slope in normal ACSF (Fig 2-11 A, Fig 2-6A). On average the ratio S2/S1 was significantly reduced by barium, like apamin (from about 2.5 ± 0.86 to 1.5 ± 0.17; Fig 2-11E). Furthermore, the S2/S1 ratio was not significantly different in barium and apamin, and approximately 1.5, indicating

that both apamin and barium blocked a similar conductance (barium and apamin sensitive) that was about equal to the leak conductance (2.5–1.5 = 1).

However, in barium there was the additional complication that the S1 conductance (leak conductance) was significantly less than in control conditions (S1= 0.12 ± 0.03 in barium vs. 0.23 ± 0.16 in normal ACSF), unlike in apamin. Thus, the finding that the S2/S1 ratio was similar in barium and apamin, actually indicates that the S2 slope itself was less in barium than apamin. Indeed, the L-Ba conductance (S2 – S1 in barium) was significantly less than the L-Ca conductance (S2 – S1 in apamin; Fig 2-11F). If anything the direct barium conductance through the L-type calcium channels should be greater than the calcium conductance (as described above; Hille, 2001); so the finding that the L-Ca conductance is instead greater than the L-Ba conductance, indicates that this L-Ca current is not purely made up of the calcium current passing through the L-type calcium channels, but also has a calcium-activated component not sensitive to apamin. That is, barium likely blocked other calcium-activated conductances, rather than just the apamin-sensitive SK current.

Surprisingly, in barium there was always a high-voltage activated large and sustained PIC (Ba PIC) that was activated above – 30 mV (2 in Fig 2-11 C), and not seen in apamin. This was activated at a distinctly higher potential than the normal low voltage activated PIC (1 in Fig 2-11 C; activated at about – 50 mV, as in nACSF or apamin), and thus remarkably discrete low and high voltage activated PICs were seen in the same cell (Fig 2-11C, 1 and 2 respectively). This high voltage activated Ba PIC produced a large

sustained plateau potential in current clamp that was very difficult to turn off (Fig 2-11D, 2), as described in detail below. This large high voltage-activated Ba PIC was an *artifact* of barium application, because it was not seen without barium even with the large depolarizations possible in apamin (Fig 2-6C). Under physiological conditions (nACSF) the cell could never be steadily depolarized past – 40mV, due to the steep SK-dependent wall, described above, and so this high voltage activate PIC has not much relevance. Probably, this high voltage activated Ba PIC was a result of a loss of inactivation of HVA calcium current (N, P/Q-type) resulting from removal of calcium from the bath, because calcium channel inactivation is known to have a strong dependence on calcium itself (calcium-dependent calcium inactivation; (Cens et al. 2005; Zong et al. 1994).

SK currents prevent uncontrollable activation of dendritic Ca PICs

The Ca PICs usually had a voltage threshold for activation (measured at electrode, in soma) that was significantly higher than the threshold for deactivation (by about 10 mV, hysteresis described above). This has previously been attributed to the dendritic nature of these currents and the inevitable poor space-clamp over these distal dendrites in very large dendritic trees of motoneurons (Hounsgaard and Kiehn 1993; Hultborn 2002). However, in nACSF this poor space clamp was not a problem, because the Ca PICs could still be fully deactivated after they were activated (Fig 2-12A&D), and thus quantified, albeit at a distance. However, in a few cells in apamin (n = 4/26) and most cells in barium (n = 4/5) the persistent calcium current (L-Ca or L-Ba) was uncontrollable, in the sense that once activated it could not be completely deactivated. This loss of control over the L-

Ca current (or L-Ba) occurred in voltage-clamp, as in Fig 2-12E, or in current-clamp, where associated plateaus could not be turned off, as in Fig 2-12B. Once we lost control over the L-Ca currents in this way, subsequent voltage evoked *smaller* L-Ca currents than before (Fig 2-13B), because a portion of the PIC was tonically activated (or inactivated). Likewise, after the first uncontrolled plateau activation with a current ramp, as second current ramp produced a smaller plateau (not shown). In these cells, we had to be very cautious in comparing the pre- and post apamin results; if the loss of control was not noticed, then the L-Ca in apamin appeared smaller than the Ca PIC before apamin, leading to the erroneous conclusion that apamin blocked the calcium current itself. Thus in the results described above only PICs measured prior to loss on control were used. We interpret the loss of control over the calcium currents after a block of SK currents as indicating that a portion of the dendritic tree distal to the electrode had gone onto an uncontrolled L-Ca mediated plateau. Why this only occurred in some cells is uncertain, though it may relate to how close the electrodes was to the center of L-Ca channel activation. In any event, these results demonstrate that the SK currents play a major physiological role of assuring that the L-Ca currents can be turned off after they are activated, because such uncontrolled PICs were not seen without apamin or barium present.

DISCUSSION

Cav1.3 calcium currents activate SK currents

Our results demonstrate that the low voltage activated persistent calcium current in spinal motoneurons activates a calcium-activated potassium current that is directly blocked by apamin and indirectly blocked by nimodipine (SK_L current). This outward SK current opposes the inward persistent calcium current, resulting in a smaller net current (Ca PIC, about 20% smaller). Previously it has been suggested that SK currents oppose persistent calcium currents in this manner (Hultborn 1999), but this had not been directly confirmed in motoneurons. Because of its low activation voltage, block with a relatively high dose of nimodipine (> 10 μM; see Results and Li and Bennett, 2003), and complete resistance to conotoxins (see Results and Li and Bennett, 2003), the persistent calcium current that activates these SK_L currents is likely mediated by the Cav1.3 channels recently characterized by Lipscomb and Xu (2001). We refer to this calcium current as the *Cav1.3 current*, for short.

High voltage activated persistent calcium currents that are, in contrast, sensitive to conotoxins have been reported in motoneurons (N, P, Q-type; Carlin et al. 2000a; McCarthy and TanPiengco 1992; Powers and Binder 2003) and these may also activate SK currents. However, the role of these persistent currents is not obvious, because during normal firing the membrane potential is held well below the spike threshold (-50 mV) by the AHPs, except for the 1 ms depolarization during each spike. Even if these currents

were of dendritic origin, their activation at above - 30 mV, means that they would not be substantially activated except transiently during the spikes, so they may only play a role during very fast firing. Furthermore, these persistent calcium currents may be partly an artifact of the patch clamp electrodes used to record them, which contained substantial calcium buffers, unlike our sharp electrodes. This may have reduced intracellular calcium sufficiently to stop the usual calcium-activated calcium channel inactivation associated with these calcium currents (N, P, and Q-type). Indeed, we found similar high-voltage-activated persistent currents in barium (and not apamin), and these are likely an artifact of substituting barium for calcium, which is known to reduced calcium channel inactivation (Cens et al. 2005). Alternatively, because this persistent inward current was only present in barium and not apamin, there may be an apamin-resistant calcium-activated potassium current that *precisely* opposes (masks) this inward current normally, though this seems unlikely because of the very large size of this barium induced inward current. The barium induced high-voltage-activated persistent inward current is activated at a distinctly higher potential (> -30 mV) than the usual low threshold persistent calcium current (Cav1.3; -50 mV threshold), and ultimately causes a peculiar second plateau riding on top of the usual low voltage activated plateau (Cav1.3 mediated) seen in motoneurons (Fig 2-11D).

We have also shown that the SK_L current is one of the major calcium-activated currents triggered by the Cav1.3 current, because a block of all calcium-activated currents produced by substituting barium for calcium has similar effects on the low-voltage-activated persistent calcium current as application of apamin alone (subthreshold to the high voltage activated currents just described; < - 40 mV). Thus, the persistent inward

current remaining in apamin, which we refer to as the L-Ca current, is a fairly good approximation of the isolated Cav1.3 current (L-Ca ~= Cav1.3), and the total persistent inward current is approximately: Ca PIC = L-Ca + SK_L current (as in Figs 2-5). However, the actions of barium are difficult to interpret quantitatively because of the greater charge carrying capability of barium compared to calcium, and changes in calcium-dependent calcium channel inactivation in barium. There remains a possibility that there are other significant calcium-activated currents triggered by Cav1.3 currents, particularly because the persistent barium conductance (L-Ba) is smaller than the persistent calcium conductance seen in apamin (L-Ca; see Results), despite the greater charge carrying capability of Ba compared to Ca. For example, there could be a calcium-activated cation current, as in some other motoneurons (Lee et al. 1996; Wu and Anderson 2000).

The SK_L current magnitude and dependence on intracellular calcium

The SK_L current is activated just after the L-Ca onset, and produces an outward current that is about 20% of the inward L-Ca current at the initial peak of the L-Ca current, making the net inward current (Ca PIC) about 20 % smaller than the L-Ca current. With time and greater depolarization (during a slow ramp), the SK_L current increases dramatically, even though the L-Ca current does not also increase. Eventually the SK_L current completely overcomes the L-Ca current (magnitude SK_L > L-Ca), so that there is no longer a net persistent inward current. At this time the high conductance of the SK_L current produces a steep increase in I-V relation (twice the leak conductance), which we

refer to as the wall, and functionally makes depolarization of the neuron past - 40 mV difficult.

The SK channel conductance is known to *not* have a voltage dependence (McLarnon 1995), but the SK_L current should at least vary linearly with voltage, increasing with the difference from the reversal potential for potassium (as for the AHP current, see Results). Also, the SK_L current should depend on the variations in intracellular Ca (McLarnon 1995), which should in principle be related to the integrated inward calcium current minus the calcium removal via buffering and pumps. Thus, the steep, greater-than-linear, increase in the SK_L current observed during the voltage ramps to -40 mV could reflect an accumulation of intracellular Ca, with calcium buffering not being able to keep pace with the maximal L-Ca current activation. In contrast, the slow decay in the SK_L current (over seconds) during a steady submaximal L-Ca current activation during a voltage step (Fig 2-8), could represent the calcium buffering overcoming the accumulation of intracellular calcium from the L-Ca current. Sometimes during a voltage ramp both of these processes occur together (Fig 2-6D): the SK_L reaches an initial peak with the L-Ca current peak and then slowly decays, but with time increases again to produce the steep SK-mediated wall.

Relationship between plateau potentials and PICs

When the Ca PICs are activated during a current ramp (Fig 2-7D) or voltage step (Li et al. 2004a), they produce a classic calcium plateau potential, due to the unstable negative-

slope region in the I-V relation (Fig 2-7A), which forces the potential to jump in an all-or-nothing manner to a greater more stable potential, above the negative slope region. Previously, (Hounsgaard and Mintz 1988) showed that these calcium plateaus are augmented by apamin, suggesting that the PICs are themselves augmented by apamin, and thus providing indirect evidence that the SK currents tend to reduce the PICs, as we have directly demonstrated. However, an increased amplitude of the PIC does not necessarily mean an increased plateau, since it is the *width* of the valley formed by the unstable negative-slope-region (in the I-V relation, Fig 2-7A&B) that determines the plateau size, and not the PIC amplitude itself (Li and Bennett 2003). Furthermore, without any changes in the PIC amplitude, a simple decrease in the overall leak conductance increases this *width*, because it takes more depolarization for the leak conductance to overcome the PIC, and this ultimately results in a larger plateau without a larger PIC (unpublished observations, Bennett and Li). So it is risky to infer changes in PICs from observations of plateaus alone. However, the present results confirm that the larger plateaus seen in apamin (Hounsgaard and Mintz, 1988) are in fact due to a block of SK currents, which in turn produces a larger PIC and a valley formed by the negative-slope region that has a greater width. In particular, this greater width in apamin occurs because the steep wall (S2 conductance) in the I-V relation is eliminated (apamin-sensitive), so greater increases in voltage are required to overcome the PIC, and ultimately this produces a greater plateau.

Calcium spikes are produced by the delayed activation of the SK_L current at the onset of an L-Ca plateau

At the onset of a calcium plateau produced by the Ca PIC there is usually at least one characteristic calcium spike in cat (Bennett et al. 1998b), turtle (Hounsgaard and Kiehn 1993) and rat (Fig 2-7). The present results demonstrate that this spike results from the slightly delayed activation of the SK_L current activation shortly after the L-Ca activation, which allows the L-Ca current to reach a transient peak (calcium spike; apamin-sensitive), after which the SK_L current hyperpolarizes the membrane potential, in what we have referred to as a CaAHP following this calcium spike. During this hyperpolarization (CaAHP), the L-Ca current must be reduced somewhat, and then the SK_L current subsides, enabling the L-Ca current to sometimes reactivate and form a second calcium spike and so on. Following about 1 to 4 calcium spikes (oscillations) L-Ca and SK_L currents reach a steady state and form a steady depolarizing current that produces a plateau potential. Interestingly, these calcium spikes occur even when the soma is voltage-clamped, suggesting that the SK_L currents are dendritic origin (see Results), which is consistent with dendritic nature to the L-Ca current (Bennett et al. 1998b; Carlin et al. 2000b; Heckman and Lee 1999a; Hounsgaard et al. 1988b).

The calcium spikes at the onset of the Ca PIC are likely important for determining the initial firing rate of the motoneuron, because they are often > 5 mV high and about 50 ms wide, and the Ca PIC is generally activated just at recruitment, particularly when activated by synaptic, rather than intracellular currents (Bennett et al. 1998b; Li et al.

2004a). Indeed, it has been argued that these spikes produce the characteristic doublets and triplets (2 - 3 spikes at about 10 ms intervals) seen at the onset of self-sustained firing that occurs in association with the Ca PIC (Gorassini et al. 1998) add 2001 human Gorassini paper too, though see other doublet mechanisms described in (Gorassini et al. 1999). However, only fast motoneurons that can fire multiple spikes in the brief calcium spike period would produce these doublets/triplets, perhaps explaining why they are common in fast hindlimb rat motoneurons (e.g. tibialis; Gorassini et al. 1999), and uncommon in the much slower tail motoneurons of the present preparation. When these doublets do occur, they should augment the net force production in muscle because of the special catch properties of muscle (Stein et al. 1988).

SK current is usually not active at rest

SK currents are not activated subthreshold to the L-Ca currents, because apamin has no effect at these membrane potentials. Thus, because Ca PICs are not usually activated at the resting membrane potential, the SK currents are also not involved in the resting membrane potential. A few cells do have their Ca currents activated at rest (Schwindt and Crill 1980), particularly when they are treated with 5-HT (Hounsgaard and Kiehn 1985), and in such cells the SK_L currents would be active at rest. Most of motoneurons do not have SK currents activated at rest (Lape and Nistri 2000; Purvis and Butera 2005).

The AHP is also mediated by SK currents, but these are activated by different calcium currents

Our results have also demonstrated that the classic post spike AHP is almost entirely mediated by an apamin-sensitive SK current (SK_{AHP}), with apamin producing a complete block of the mAHP and only leaving the small transient fAHP (see results). This is to be expected, based on previous results from other neurons and motoneurons, where the mAHP is mediated by SK currents and the fAHP mediated by apamin-resistant BK currents (Schwindt et al. 1988; Viana et al. 1993). Furthermore, our results demonstrate that these SK_{AHP} currents are activated by the fast transient high-voltage-activated calcium currents (conotoxins-sensitive N, P and Q-type) triggered during the action potential, consistent with results of previous studies (Pineda et al. 1998; Viana et al. 1993; Williams et al. 1997). The classic high-voltage activated L-type calcium currents (e.g. Cav1.2, as opposed to Cav1.3) do *not* contribute substantially to the SK_{AHP} (nimodipine-resistant), probably because of their slow kinetics (Lipscombe et al. 2004). Interestingly, these AHP results indicate that the calcium that activates the SK_{AHP} current is completely different from the calcium that activates the SK_L current, even though both of these SK currents are apamin sensitive. That is, only low voltage-activated L-type calcium currents (Cav1.3), and not N, P and Q-type calcium currents, are involved in the Ca PIC and associated SK_L currents, because conotoxins do not affect these, whereas nimodipine blocks the Ca PIC and SK_L (see above).

There is no sAHP in motoneurons, but the SK_L current is a similar phenomenae

In some neurons, like hippocampal neurons (Tombaugh et al. 2005), there is very slow AHP (sAHP) that follows a train of action potentials. This has been shown to be mediated by high-voltage activated calcium currents and the L-type calcium currents activating SK current (Pineda et al. 1999). Motoneurons do not have this sAHP, but they do have an L-type calcium current that produces a depolarizing after potential (L-Ca plateau), following firing (Fig 2-2A), and this afterpotential is augmented by apamin, indicating that SK_L current oppose the L-Ca current. However, the SK_L current is not larger than the L-Ca current, and a net depolarization is always produced (afterpotential). Had the SK_L current exceeded the L-Ca current, a net hyperpolarization would have occurred, producing a sAHP like in hippocampal cells. Thus, the difference between cells that have an sAHP and cells that have an afterpotential may simply be a matter of the relative balance of SK_L and L-Ca currents.

SK_{AHP} stops all-or-nothing PIC activation, whereas SK_L does not

When spikes are blocked with TTX, there is a rapid all-or-nothing activation of the L-Ca current that forms a plateau (as described above), and while the SK_L currents reduce the net PIC, they do not themselves prevent this all-or-nothing activation of the PIC. In contrast, during firing, the additional SK currents produced by the AHP (SK_{AHP}) do prevent (or at least slow) the rapid all-or-nothing PIC activation seen in TTX. That is, the

accumulated hyperpolarization from the AHP effectively holds (clamps) the membrane potential below the firing threshold (- 50 mV), limiting the full PIC activation. The potential only exceeds this firing threshold for 1 ms or so each spike, and the L-Ca current does not respond to such small transients (Fig 2-8 and Li and Bennett 2003). Thus, from the stand point of the slow L-Ca current, the membrane is indeed clamped below the firing level. When apamin selectively blocks the AHP, the L-Ca is instead activated in an all-or-nothing manner, and this causes extremely high firing rates, followed by a very large plateau potential after firing stops (Fig 2-2B), confirming the critical role of the AHP in preventing all-or-nothing PIC activation. Furthermore, these results are consistent with the classic notion that the AHP limits the maximum firing rate (Kernell 1965).

Role of SK current in the primary, secondary and tertiary ranges of F-I relation

As just described, when AHPs are present (without apamin) the membrane potential is effectively clamped to stay below the firing threshold, and thus the Ca PIC activation is initially held at or below the level achieved at recruitment. However, the firing threshold increases somewhat with increased firing rate (Schwindt and Crill 1982), and so further Ca PIC activation is possible as the firing rate increases with increased current injection. This extra current from the Ca PIC causes further increases in firing rate enabling still further increases in the Ca PIC and so on. Ultimately, this activation of the Ca PIC leads to the steep increase in firing rate that is known as the secondary range of firing in the frequency-current relation (F-I relation; i.e., secondary range is nimodipine-sensitive; Li

et al. 2004a). After a sufficient increase in firing rate (and firing threshold), the Ca PIC is able to become relatively fully activated (or at least saturated), and further increases in current only gradually increase the firing, and this region is known as the tertiary range (very shallow F-I slope region; nimodipine-sensitive; Li et al. 2004a).

In some cells the Ca PIC is not activated at recruitment during intracellular current injection (unlike in Fig 2-2), and in these cells the firing increases with only a shallow slope in the F-I relation (in classic primary range), until the Ca PIC activation starts, and then produces a secondary range. However, this primary range firing is an artifact of current injection, and never occurs when the cell is activated by synaptic inputs alone (Bennett et al. 1998a; Li et al. 2004a; Li et al. 2004b). Instead, with synaptic inputs neurons start firing either in the secondary range (with Ca PIC only gradually activated), or immediately in the tertiary range (with Ca PIC saturated at recruitment; (Bennett et al. 1998b; Li et al. 2004a). Even with current injection, many rat motoneurons also start firing immediately in the tertiary range at recruitment (e.g. Fig 2-2A). In these cells, there is no rapid acceleration in firing after recruitment, but there is a steady Ca PIC present because this current produces pronounced self-sustained firing (nimodipine-sensitive; Li et al. 2004) that continues even in the presence of hyperpolarizing currents well below the recruitment current (as in Fig 2-2). Likely, in these cells the Ca PIC is saturated at a fixed level at recruitment, though this level may not be the maximum Ca PIC activation, because the SK currents limit (clamp) the depolarization, and apamin seems to enable a larger net depolarization/plateau in these cells (Fig 2-2B).

Voltage-clamp also prevents all-or-nothing Ca PIC activation, like the AHP

When the membrane potential at the soma is directly voltage-clamped, the Ca PIC is also only gradually activated during an increasing voltage ramp, because the Ca PIC are prevented from fully activating by the voltage-clamp, at least in the dendrites close enough to the soma to control with the clamp. This direct voltage-clamp is similar to the effective clamp of the membrane potential by the AHP currents during firing (just described). We find that for these neurons good voltage clamp of the Ca PIC (with less than a few mV clamp error) is obtained with a clamp gain of at least 1 nA/mV (see Methods), which corresponds to a conductance introduced by the clamp of 1 μS. In comparison, during firing the AHPs themselves provide an SK current with a conductance of about 0.2 μS, and the SK_L provides a similar conductance at its maximum (0.2 μS). Thus, these SK currents provide an effective clamp of the Ca PICs that is poor in relation to our direct voltage clamp, but nonetheless, they do prevent full PIC activation.

Slow firing in apamin

The AHP duration has classically been thought to determine the maximum interspike interval, and thus determine the minimum firing rate, and indeed this is the case in motoneurons of pentobarbital anaesthetized cats or acutely spinalized rats without persistent sodium currents (Na PICs; Li et al. 2004a, Kernell, 1965). However, recently it

has been shown that motoneurons that possess large subthreshold Na PICs are able to fire at much lower rates (and thus longer intervals) than determined by the AHP duration (Li et al. 2004a; Harvey et al. 2005a). This slow firing is often very regular, and occurs even in the absense of synaptic noise. In particular, when these Na PICs are large enough to produce a negative slope region in the I-V relation, then these Na PIC cause slow intrinsic oscillations (1 - 4 Hz) in the membrane potential near the firing threshold, and these oscillations ultimately trigger the slow firing. Each cycle of this oscillation take the form of an initial slow depolarization (ramp; double arrow in Fig 2-2D) followed by a faster depolarization (acceleration; * in Fig 2-2D) which ultimately triggers a spike. Following each spike an AHP occurs that deactivates the Na PIC transiently, and then the Na PIC is reactivated again with the characteristic ramp&acceleration profile. This ramp&accelerate profile is resistant to nimodipine (not L-Ca mediated) and blocked by a low dose of TTX that blocks the Na PIC without affecting the sodium spike, and thus is Na PIC mediated (Li et al. 2004a). The present results indicate that such Na PIC mediated slow firing can still occur when the mAHP is blocked by apamin. In this case the fAHP seems to be sufficient to deactivate the Na PIC following each spike, and the same Na PIC mediated ramp&acceleration depolarization profile follows after each fAHP, though the slow firing is not as robust as with a mAHP present. Thus, slow firing appears to continue with the same underlying Na PIC oscillation, but with the mAHP no longer interposed between the spike and the Na PIC activation. Importantly, in apamin this firing that is mediated by the Na PIC oscillations is *not* restricted to very slow rates, and occurs at faster rates with interspike intervals much less than the usual mAHP duration (Fig 2-2B). Thus, *Na PIC oscillations must participate in determining the*

interspike interval when firing at all rates; its effect is just more obviously separated from the mAHP at very low rates.

Possible spatial location of SK channels

The spatial location of the SK currents underlying the AHP (SK_{AHP} currents) is uncertain, though these are likely close to the location of the action potential initiation and associated high-voltage-activated calcium channels, because of the speed with which the AHP is initiated following the spike. Thus, these SK_{AHP} currents are likely located close to the soma and proximal dendrites, where the spike is initiated (Oomura and Maeno 1963). Thus, the AHP current are likely located near the intracellular electrode, consistent with the very linear AHP *vs* potential relation which has a reversal potential at only -81 mV (Fig 2-4B). In contrast, the SK_L currents may not be as closely localized/associated to the L-type calcium currents that activate them during plateau potentials, because SK_L initiation is delayed about 100 ms after the onset of the L-type calcium current (see Results). The L-Ca currents themselves arise from the dendrites, with the major L-Ca activation likely occurring at least 300 um distally to the soma (half of a space constant; Bennett 1998b). Thus, it could be that the SK_L currents are more proximal than the majority of the L-Ca currents. Indeed, an intriguing hypothesis is that the *same* population of SK channels produce the SK_{AHP} and the SK_L currents. In this way the much larger delay in the SK_L current, in relation to the SK_{AHP} current, could arise from these SK channels being closer to the spike initiation zone (cell body) than the majority of the

L-type calcium channels underlying the L-Ca. However, while this is an attractive idea, there are several problems to consider. First, we do not know much about the relative spatial location of L-type Cav1.3 channels (L-Ca associated) and SK channels on motoneurons, though we do know that L-type Cav1.2 channels are closely associated with SK channels in other neurons (Bowden et al. 2001). Second, the SK_L oscillations seen in voltage clamp suggest unclamped dendritic SK currents. Third, we have found that the SK_L current play a major role in assuring that L-Ca currents can be deactivated (Fig 2-12 and 2-13), and for this it seems especially important to have SK_L currents on the most distal, least controllable dendrites where the L-Ca exist. Perhaps the SK currents are both proximal and distally to the L-Ca current, but not immediately co-localized.

Effect of chronic spinal cord injury on the SK_L current

The present results indicate that both motoneurons of acute and chronic spinal rats have SK_L currents activated by the Cav1.3 currents (L-Ca current), and together these form a net persistent inward current (Ca PIC). The whole sacrocaudal spinal cord of normal rats was maintained *in vitro* in the present experiment, and this *in vitro* preparation was termed acute spinal because of the necessary transection needed to remove the spinal cord. Such acute injury has been shown to reduce the motoneuron excitability, and in particular reduce PICs (Hounsgaard et al. 1988a), and thus it is not surprising that the L-Ca current in acute spinal rats is small (with no negative slope region; Harvey et al. 2005a, b). With chronic spinal cord injury the motoneurons somehow adapt and recover

their excitability, and in particular exhibit large PICs (Li and Bennett 2003), consistent with the large L-Ca currents seen in the present chronic spinal rats (see Results). We do not know about the corresponding SK_L current in the intact rat, though it is likely that these are present, because there is good evidence that intact animals (and humans) have persistent calcium currents (Ca PICs) that help sustain motor unit firing. Furthermore, qualitatively the PICs in spinal cord intact decerebrate cats (Lee and Heckman 1998a) are similar to those of chronic spinal rats (i.e. both have a pronounced negative slope region that produces plateaus), and so the L-Ca and SK_L current likely most closely approximate the currents seen in the spinal cord intact animal.

Interestingly, the SK_L current is not significantly bigger in chronic spinal compared to acute spinal rate, despite the much larger L-Ca current in chronic spinal rats. Thus, there appears to be less availability of SK_L channels in chronic spinal rats, compared to acute spinal rats, because the larger L-Ca current does not activate larger a SK_L current, in contrast to what would be expected if the SK channels remained unchanged. Thus, the larger net Ca PIC (L-Ca + SK_L) seen in chronic spinal rats, compared to acute spinal, may in small part be due to this reduced SK channel availability. However, similar conclusions can not be drawn from the SK_{AHP} results. The AHP and associated SK_{AHP} current and conductance is not different in acute and chronic spinal rats (see Results), and furthermore the spikes that trigger the AHP are not different in acute and chronic spinal rats (Li et al. 2004a). So there is no change in availability of the SK_{AHP} current with chronic injury. Although, the reason for this discrepancy between the changes in SK_L and

SK_{AHP} currents with chronic injury are uncertain, it provides indirect evidence that these two SK currents are mediated by different populations of SK channels.

Figure 2-1

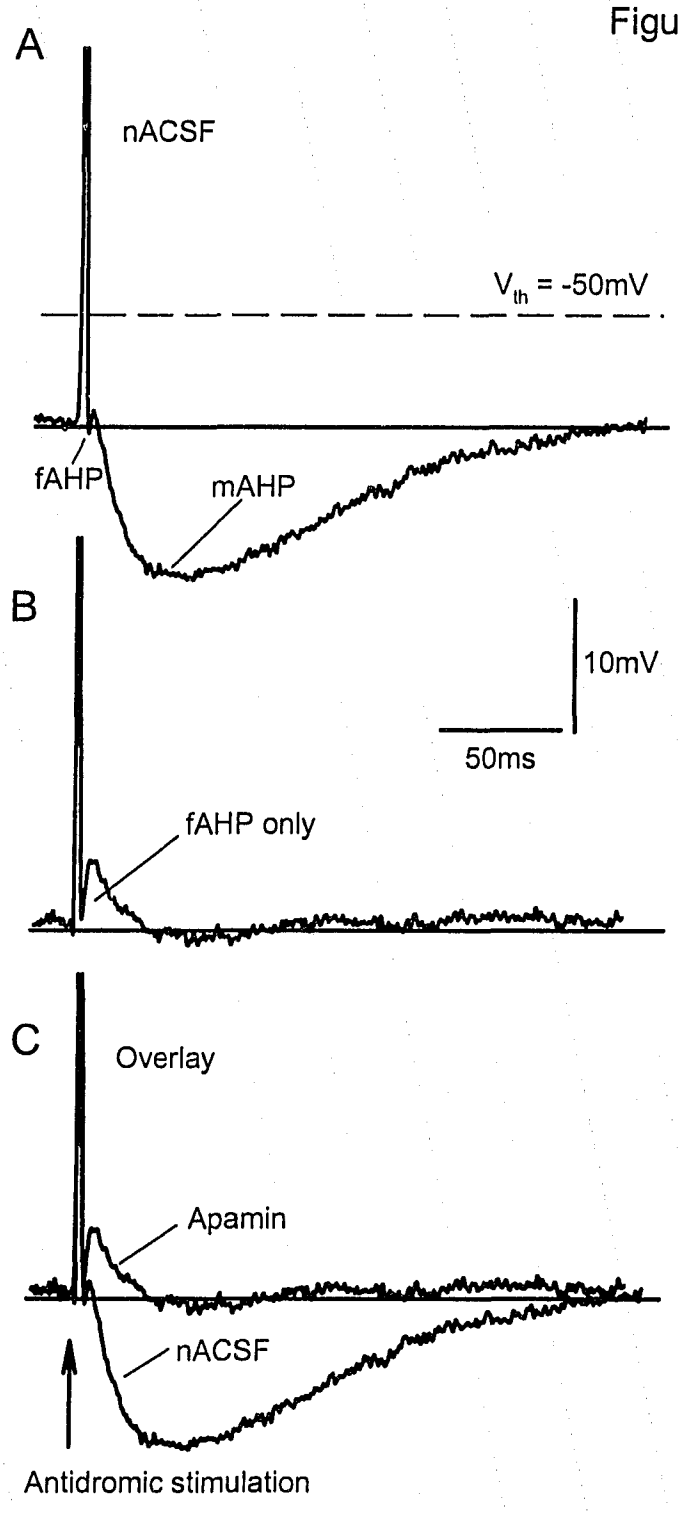

Figure 2-1. Apamin blocks the mAHP following an antidromic spike. A: A spike was induced by antidromic stimulation with following fAHP and mAHP, recorded from a motoneuron after chronic injury. B: Apamin totally blocks the mAHP, but did not decrease the fAHP. C: Figure shows the overlay of the motoneuron response before and after apamin.

Figure 2-2

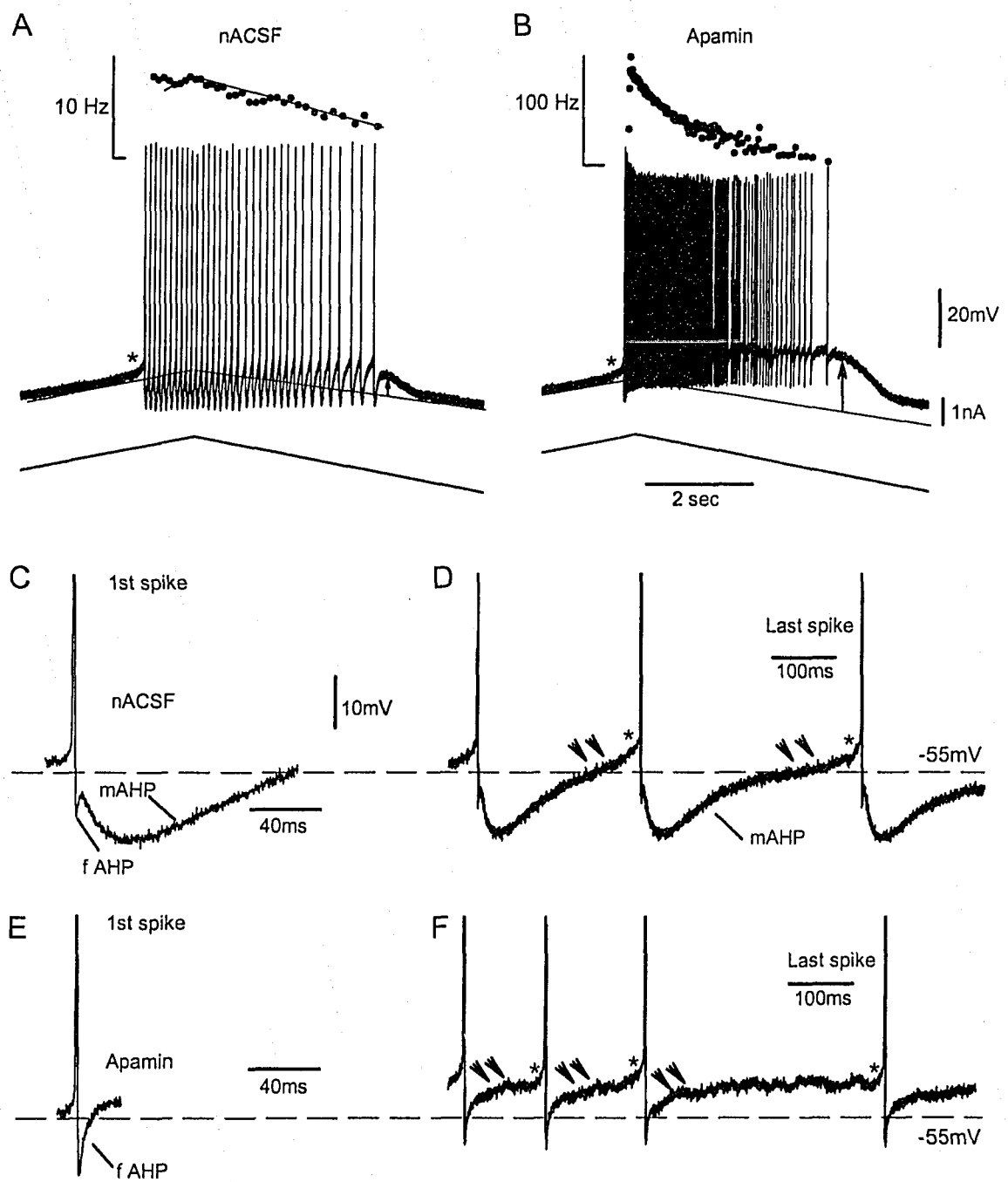

Figure 2-2. The effect of apamin on repetitive firings, recorded from a motoneuron after chronic injury. A: The cell fires repetitively on an increasing current ramp with a frequency less than 10 Hz and a small plateau. B: In apamin, the cell fires with an initial frequency higher than 100 Hz and gradually decreased, with a bigger plateau following the firing. C: The first spike from figure A shows fAHP and a full mAHP. D: The last spikes from figure A also shows plateau. E: The mAHP following the first spike was eliminated by apamin. F: Apamin also totally blocks the mAHPs after the last spikes. * shows the Ca/Na PIC initiated before a spike. Double arrow shows the Na-dependent ramp&acceleration profile.

Figure 2-3

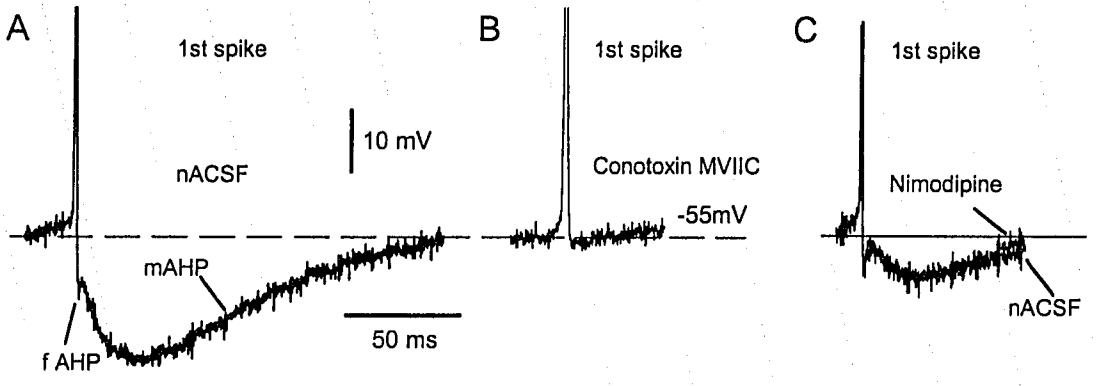

Figure 2-3. Both fAHP and mAHP are blocked by N-type and P/Q-type calcium channel blocker conotoxin MVIIC, but not affected by L-type calcium channel blocker nimodipine. A: a full spike with fAHP and mAHP. B: Both the fAHP and the mAHP were eliminated by conotoxin MVIIC. C: Overlay of the cell response before and after nimodipine, the mAHP was not affected by nimodipine.

Figure 2-4

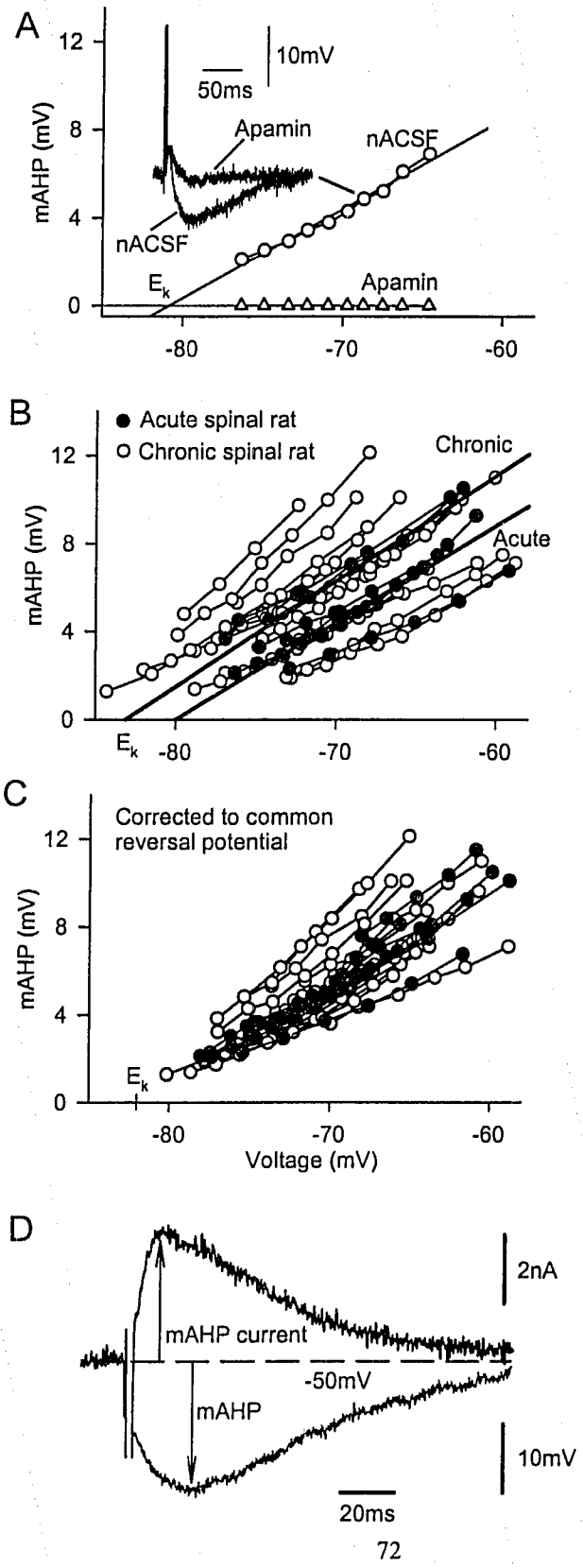

Figure 2-4. The amplitude of mAHP increases linearly with higher membrane potential. A: The amplitudes of mAHPs are voltage-dependent and increases linearly with higher membrane potential. Apamin completely blocked the mAHPs at any potential. An overlay of the mAHP before and after apamin is also shown. B: The relationship of mAHP amplitudes vs. voltage were recorded from 15 cells after chronic spinal rats and 7 cells from normal rats. Thick straight lines shows the average potassium reversal potential for motoneurons from chronic spinal rats and normal rats respectively. C: The responses were corrected to an overall potassium reversal potential. D: Black trace show a mAHP current recorded in voltage clamp mode; gray trace shows the corresponding mAHP in current clamp mode.

Figure 2-5

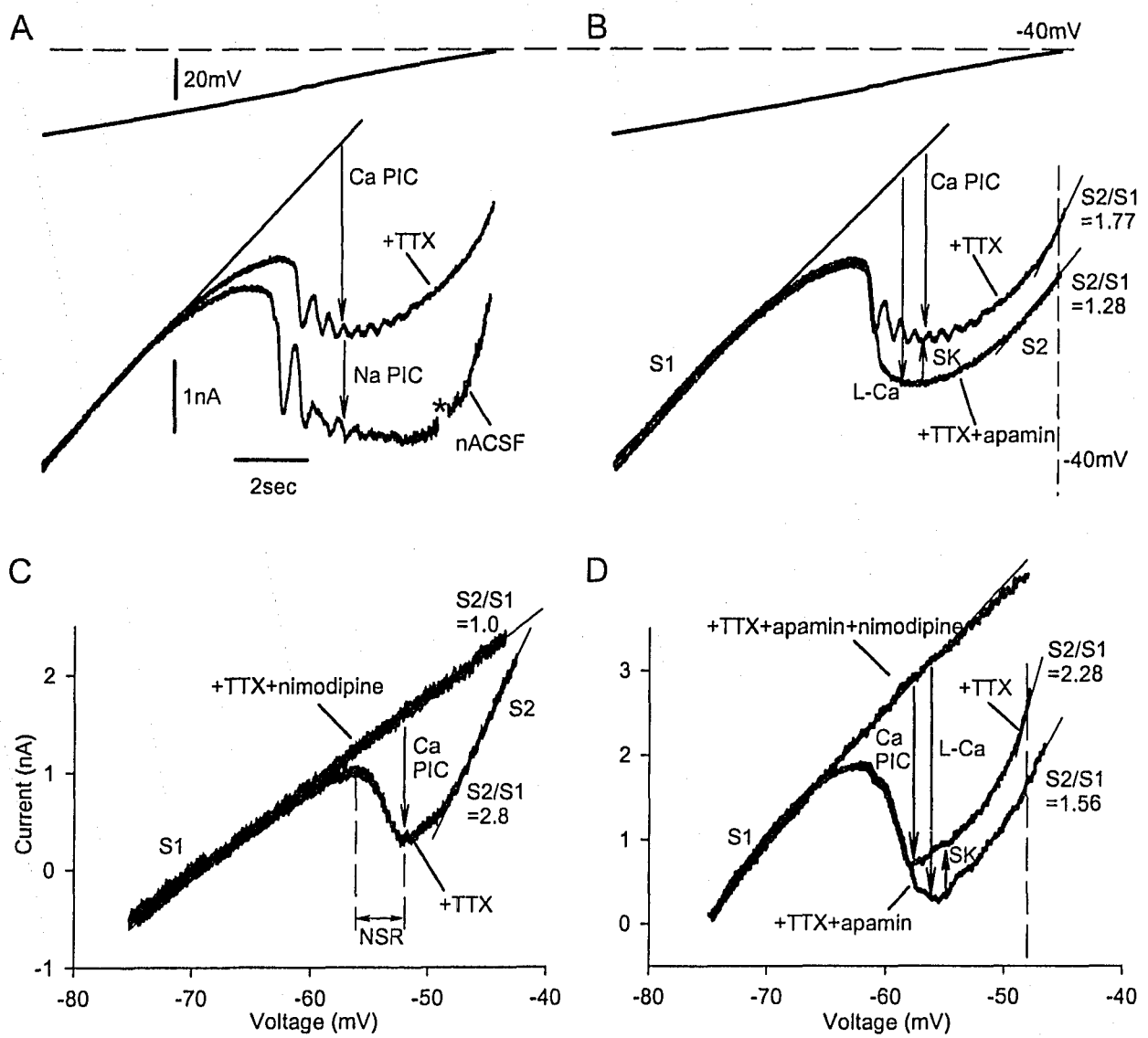

Figure 2-5. Apamin increases the Ca PIC by blocking SK current and nimodipine eliminates both Ca PIC and SK current, recorded in a motoneuron after chronic injury. A: In voltage clamp mode, TTX decreased the total PIC by blocking Na PIC and left a Ca PIC. B: Apamin increased revealed L-Ca current from the Ca PIC by eliminating the SK current. The S2 slope is reduced by apamin. C: TTX and nimodipine blocks any current in the recorded voltage range and made S2 equal to S1. D: TTX and apamin revealed the L-Ca current and lower S2 slope, further application of nimodipine blocked the L-Ca current and made S2 equal to S1 by eliminating any additional conductance.

Figure 2-6

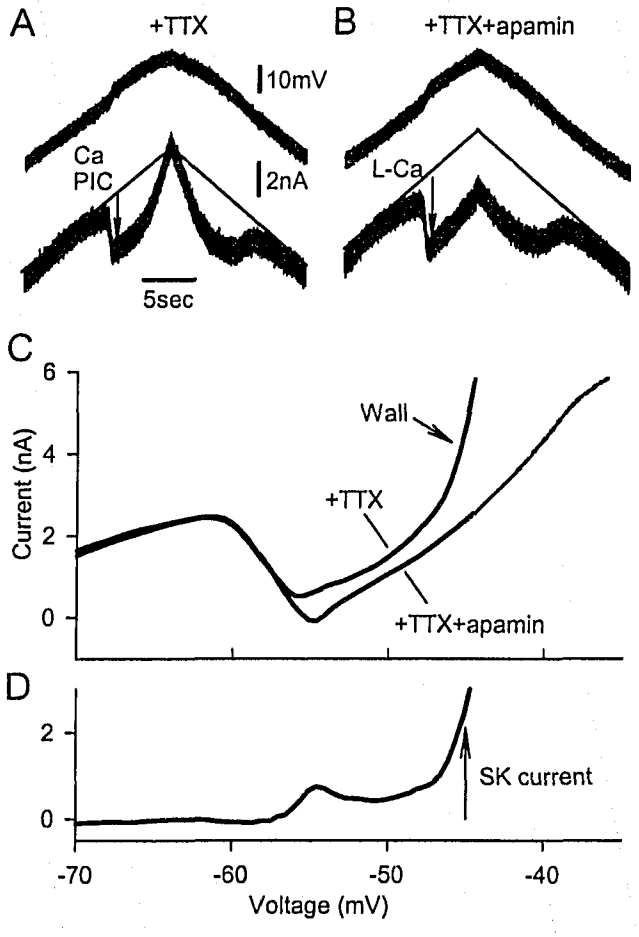

Figure 2-6. SK current increases with higher potential; apamin eliminates the high SK conductance "wall". A: In some cells, SK current increases dramatically with up-ramping voltage and made a steep SK conductance "wall". B: The "wall" was eliminated by apamin. C: The I-V relationship overlay before and after apamin. At an equal voltage, the SK current was reduced; an equal current can be reached only at a higher voltage (gray trace). D: The relationship of pure SK current vs. voltage before apamin was demonstrated.

Figure 2-7

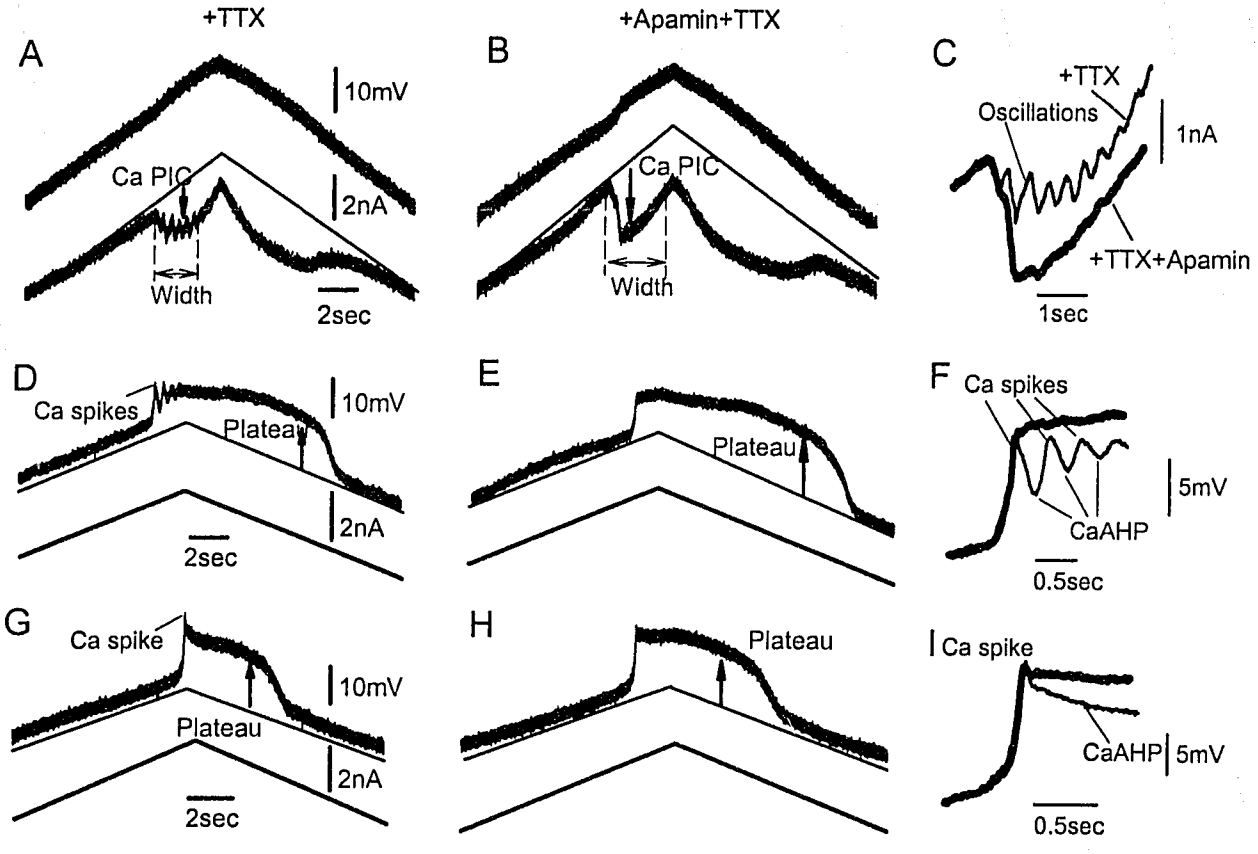

Figure 2-7. Apamin increases and widens the Ca PIC, and increases the height and duration of the Ca plateau as well. A: A voltage clamp response recorded from a motoneuron after chronic injury. B: Apamin increased the PIC amplitude and width. C: The peak of the PICs are overlaid and shown in large scale. The PIC is larger and the Ca oscillations are gone. D: A Ca plateau induced by a ramping current was shown, recorded from the same motoneuron with figure A. E: Apamin blocked the Ca spikes at the onset of the plateau, increased the amplitude and duration of the Ca plateau. F: The onset part of the Ca plateaus were overlaid and shown in large scale. G: A Ca plateau can also be induce in a normal motoneuron with a current ramp. H: Apamin blocked the Ca spike and increase the Ca plateau in normal cells as well. I: The onset part of the Ca plateaus recorded from normal motoneuron were overlaid and shown in large scale.

Figure 2-8

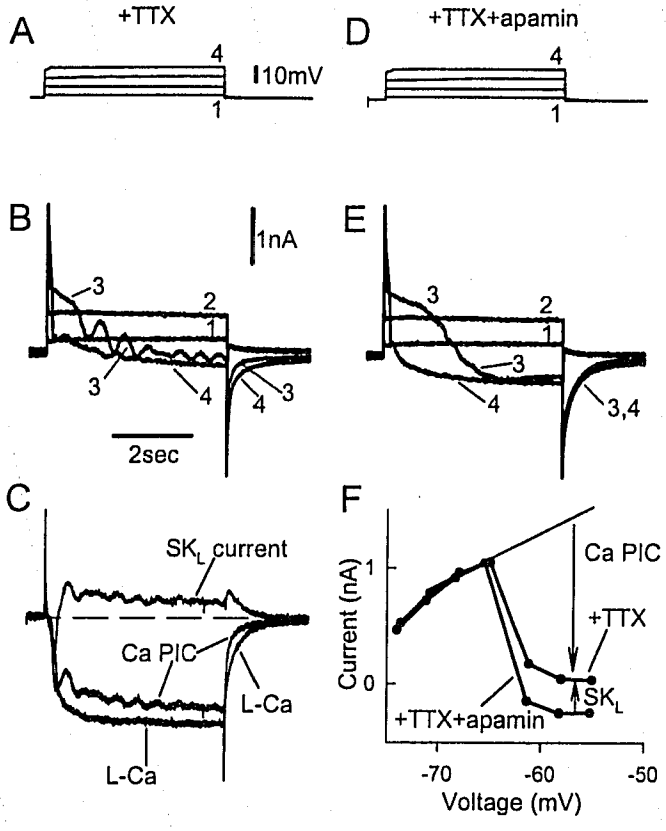

Figure 2-8. Current responses to voltage steps before and after apamin. A&B: Long square voltage steps and corresponding current responses recorded in a motoneuron from chronic spinal rat. D&E: After apamin, the currents were recorded at matched voltage steps from the same motoneuron. C: Two current traces responding to an equal potential were overlaid (not shown in figure B&E) and the SK_L current was calculated by subtracting the L-Ca current from the Ca PIC. Also note that the tail current after apamin lasts longer. F: The I-V relationships of current to voltage steps before and after apamin are compared and the SK_L current is revealed by subtracting between the two traces.

Figure 2-9

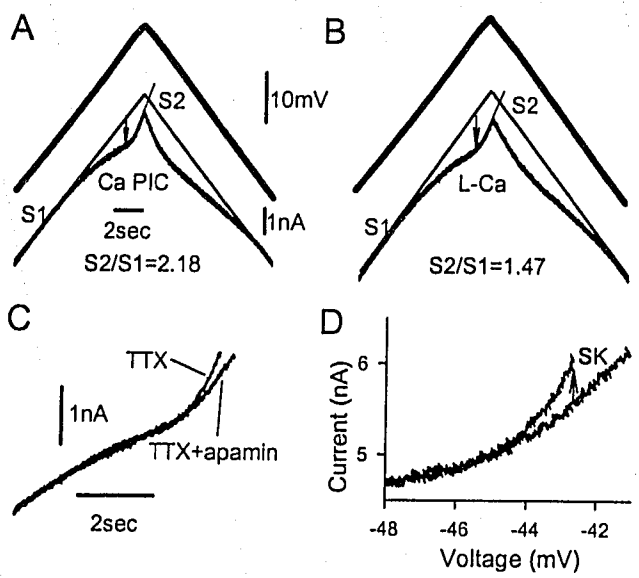

Figure 2-9. The effect of apamin on Ca PICs in normal motoneurons. A: Ca PIC can be induced in normal motoneurons with a voltage clamp, and shows a steeper S2 slope than S1 slope. Usually no negative slope regions (NSR) are presented in normal motoneurons. B: Apamin increased the Ca PIC by blocking the SK current and revealed an L-Ca, apamin also reduced the S2/S1 ratio as in motoneurons after chronic injury. C: The SK current and SK conductance can be demonstrated by overlaying the current responses before and after apamin. D: In I-V relationship, it is shown that an SK current was blocked by apamin, also, the SK current and conductance increased with higher potential.

Figure 2-10

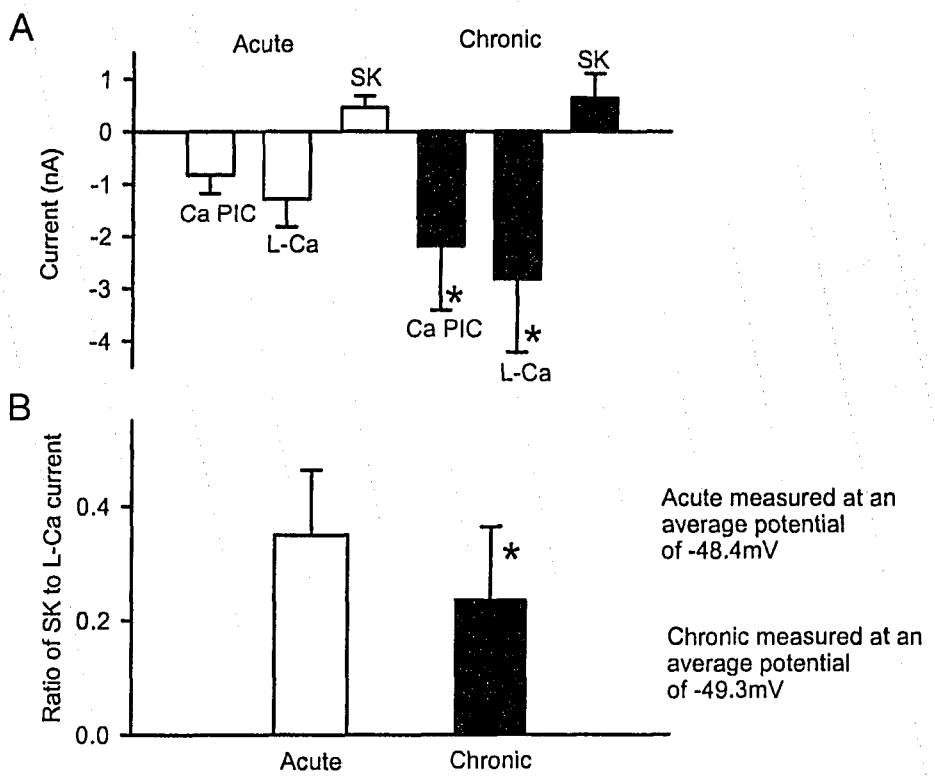

Figure 2-10. The amplitudes of each current in motoneurons after acute and chronic injury were summarized and compared. A: The amplitudes of Ca PIC and L-Ca are significantly higher in motoneurons after chronic injury than in normal cells. The SK current is also larger in cells after chronic injury, but not significantly. B: The ratio of SK to L-Ca current is significantly higher in normal cells than in cells after chronic injury. The amplitudes of the currents were recorded at a comparable average potential (-48.4mV for acutes and -49.3mV for chronics).

Figure 2-11

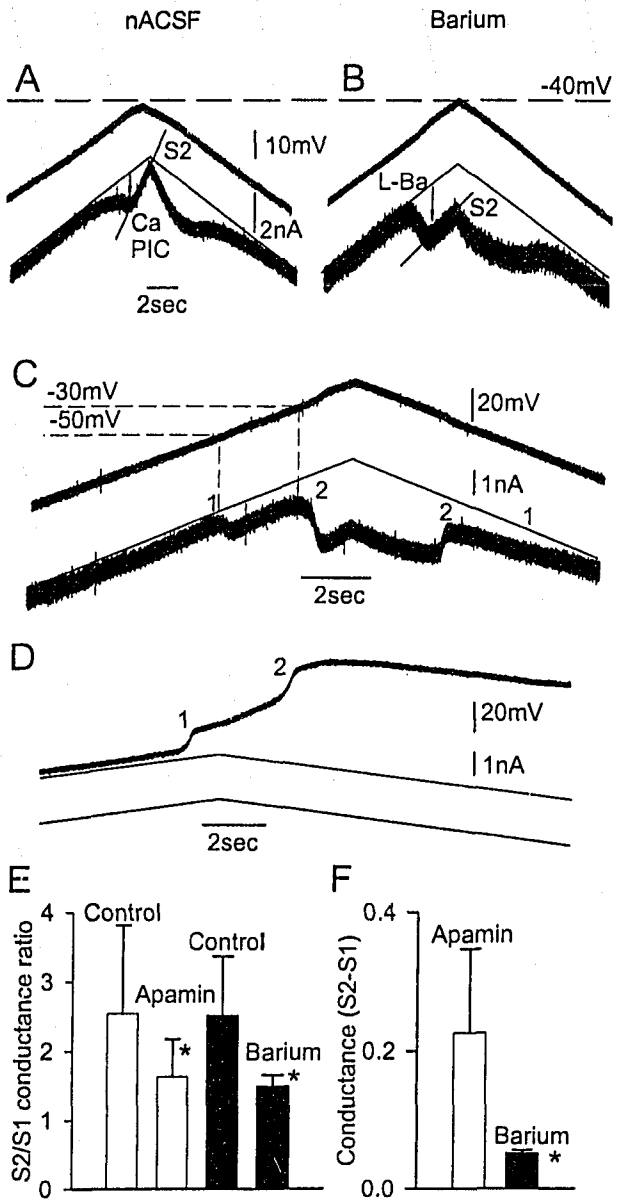

Figure 2-11. The SK current can also be blocked by replacing Ca^{++} with Ba^{++} in the nACSF. A: A Ca PIC and steep S2 were induced by increasing potential in a voltage clamp. B: By replacing Ca^{++} with Ba^{++}, the PIC is increased and the S2/S1 is lowered. C: In voltage clamp mode, two Ba PICs are induced, one has a lower threshold (near -50mV) and the other has a higher threshold (near -30mV). D: In a corresponding current clamp, a double-plateau can be activated and last for a long time. E: Both apamin and Ba can significantly reduce the S2/S1 slope ratio; the ratio is very similar, either apamin or Ba is used to block the SK current. F: Apamin blocked a conductance which is significantly higher than the conductance blocked by Ba.

Figure 2-12

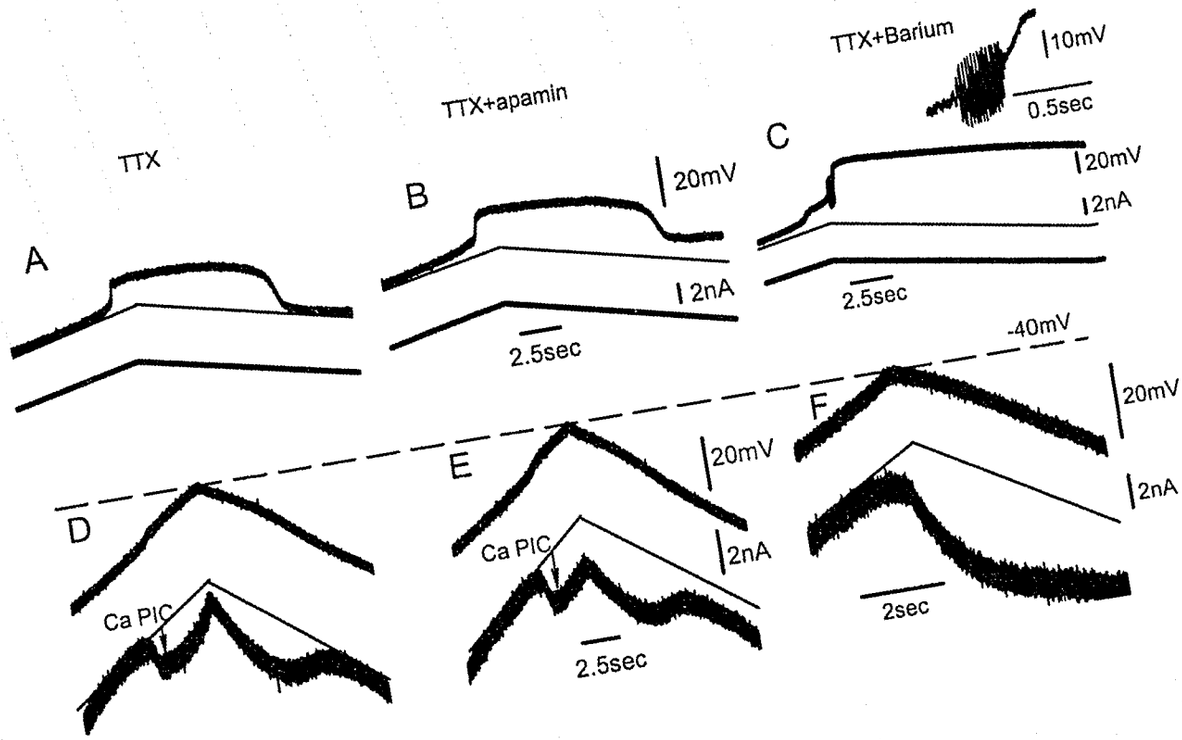

Figure 2-12. The blockade of the SK channel causes a loss of control of the clamps. A&D: In TTX, a good control of the clamps were shown, i.e. the activated currents were totally de-activated either in current clamp mode or voltage clamp mode. B&E: With the presence of TTX and apamin, sometimes, the activated current can not be fully de-activated by lowering the membrane potential. C&F: In Ba, the control over the currents are more difficult and might lost most of the control of the clamp. Figure C also shows a sequence of Ba spikes activated at the onset of the second Ba plateau, shown in large scale as well.

Figure 2-13

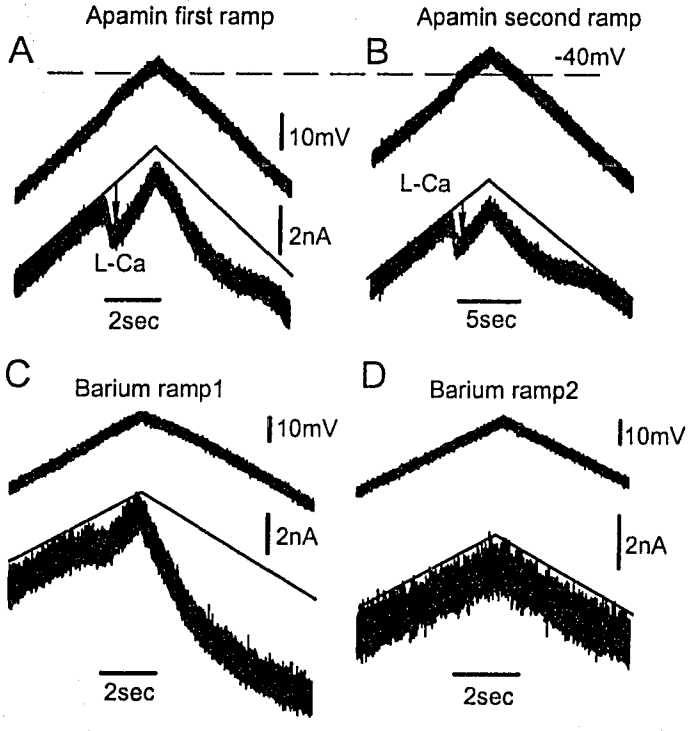

Figure 2-13. The recorded PICs are smaller if a loss of control over the current happens. A: In apamin, an L-Ca is activated but not fully de-activated due to a loss of control over the current during the first ramp. B: In the following ramp, the recorded L-Ca became smaller compared to the PIC in the first ramp. C: With Ba to block the SK current, a Ba PIC can be activated and kept on. D: In the second ramp, no PIC can be induced any more; but a huge negative bias current is needed to keep the membrane potential stable.

REFERENCES

Bennett DJ, Gorassini M, Fouad K, Sanelli L, Han Y, and Cheng J. Spasticity in rats with sacral spinal cord injury. *J Neurotrauma* 16: 69-84, 1999a.

Bennett DJ, Gorassini MA, and Siu M. In vitro preparation to study spasticity in chronic spinal rats. *Soc Neuroscience Abst* 25: 1394, 1999b.

Bennett DJ, Hultborn H, Fedirchuk B, and Gorassini M. Short-term plasticity in hindlimb motoneurons of decerebrate cats. *J Neurophysiol* 80: 2038-2045, 1998a.

Bennett DJ, Hultborn H, Fedirchuk B, and Gorassini M. Synaptic activation of plateaus in hindlimb motoneurons of decerebrate cats. *J Neurophysiol* 80: 2023-2037, 1998b.

Bennett DJ, Li Y, Harvey PJ, and Gorassini M. Evidence for plateau potentials in tail motoneurons of awake chronic spinal rats with spasticity. *J Neurophysiol* 86: 1972-1982, 2001a.

Bennett DJ, Li Y, and Siu M. Plateau potentials in sacrocaudal motoneurons of chronic spinal rats, recorded in vitro. *J Neurophysiol* 86: 1955-1971, 2001b.

Bowden SE, Fletcher S, Loane DJ, and Marrion NV. Somatic colocalization of rat SK1 and D class (Ca(v)1.2) L-type calcium channels in rat CA1 hippocampal pyramidal neurons. *J Neurosci* 21: RC175, 2001.

Buschges A. The Physiology of Sensory Cells in the Ventral Scoloparium of the Stick Insect Femoral Chordotonal Organ. *J Exp Biol* 189: 285-292, 1994.

Carlin KP, Jiang Z, and Brownstone RM. Characterization of calcium currents in functionally mature mouse spinal motoneurons. *Eur J Neurosci* 12: 1624-1634, 2000a.

Carlin KP, Jones KE, Jiang Z, Jordan LM, and Brownstone RM. Dendritic L-type calcium currents in mouse spinal motoneurons: implications for bistability. *Eur J Neurosci* 12: 1635-1646, 2000b.

Cens T, Rousset M, Leyris JP, Fesquet P, and Charnet P. Voltage- and calcium-dependent inactivation in high voltage-gated Ca(2+) channels. *Prog Biophys Mol Biol*, 2005.

Dutia MB and Johnston AR. Development of action potentials and apamin-sensitive after-potentials in mouse vestibular nucleus neurones. *Exp Brain Res* 118: 148-154, 1998.

Enomoto K, Furuya K, Maeno T, Edwards C, and Oka T. Oscillating activity of a calcium-activated K+ channel in normal and cancerous mammary cells in culture. *J Membr Biol* 119: 133-139, 1991.

Gorassini M, Bennett DJ, Kiehn O, Eken T, and Hultborn H. Activation patterns of hindlimb motor units in the awake rat and their relation to motoneuron intrinsic properties. *J Neurophysiol* 82: 709-717, 1999.

Gorassini MA, Bennett DJ, and Yang JF. Self-sustained firing of human motor units. *Neurosci Lett* 247: 13-16, 1998.

Gorassini MA, Knash M, Harvey PJ, Bennett DJ, and Yang JF. Role of motoneuron plateau potentials in the generation of involuntary muscle activity after spinal cord injury. *Brain* 127: 2247-2258, 2004.

Harvey PJ, Li Y, Li X, and Bennett DJ. Persistent sodium currents and repetitive firing in motoneurons of the sacrocaudal spinal cord of adults. 2005. Submitted to J Neurophysiol.

Harvey PJ, Li Y, Li X, and Bennett DJ. Serotonin facilitates persistent sodium currents in motoneurons, and spinal cord transection leads to a supersensitivity to serotonin. 2005. Submitted to J Neurophysiol.

Harvey PJ, Li Y, Li X, and Bennett DJ. Endogenous monoamines are essential for persistent sodium currents and repetitive firing in rat spinal motoneurons. 2005. In preparation.

Heckman CJ and Lee RH. The role of voltage-sensitive dendritic conductances in generating bistable firing patterns in motoneurons. *J Physiol Paris* 93: 97-100, 1999a.

Heckman CJ and Lee RH. Synaptic integration in bistable motoneurons. *Prog Brain Res* 123: 49-56, 1999b.

Hounsgaard J, Hultborn H, Jespersen B, and Kiehn O. Bistability of alpha-motoneurones in the decerebrate cat and in the acute spinal cat after intravenous 5-hydroxytryptophan. *J Physiol* 405: 345-367, 1988a.

Hounsgaard J and Kiehn O. Ca++ dependent bistability induced by serotonin in spinal motoneurons. *Exp Brain Res* 57: 422-425, 1985.

Hounsgaard J and Kiehn O. Calcium spikes and calcium plateaux evoked by differential polarization in dendrites of turtle motoneurones in vitro. *J Physiol* 468: 245-259, 1993.

Hounsgaard J and Kiehn O. Serotonin-induced bistability of turtle motoneurones caused by a nifedipine-sensitive calcium plateau potential. *J Physiol* 414: 265-282, 1989.

Hounsgaard J, Kiehn O, and Mintz I. Response properties of motoneurones in a slice preparation of the turtle spinal cord. *J Physiol* 398: 575-589, 1988b.

Hounsgaard J and Mintz I. Calcium conductance and firing properties of spinal motoneurones in the turtle. *J Physiol* 398: 591-603, 1988.

Hultborn H. Plateau potentials and their role in regulating motoneuronal firing. *Adv Exp Med Biol* 508: 213-218, 2002.

Hultborn H. Plateau potentials and their role in regulating motoneuronal firing. *Prog Brain Res* 123: 39-48, 1999.

Keen JE, Khawaled R, Farrens DL, Neelands T, Rivard A, Bond CT, Janowsky A, Fakler B, Adelman JP, and Maylie J. Domains responsible for constitutive and Ca(2+)-dependent interactions between calmodulin and small conductance Ca(2+)-activated potassium channels. *J Neurosci* 19: 8830-8838, 1999.

Kernell D. The limits of firing frequency in cat lumbosacral motoneurones possessing different time course of afterhyperpolarization. *Acta Physiol Scand* 65: 87-100, 1965.

Kiehn O and Eken T. Prolonged firing in motor units: evidence of plateau potentials in human motoneurons? *J Neurophysiol* 78: 3061-3068, 1997.

Lancaster B, Nicoll RA, and Perkel DJ. Calcium activates two types of potassium channels in rat hippocampal neurons in culture. *J Neurosci* 11: 23-30, 1991.

Lape R and Nistri A. Current and voltage clamp studies of the spike medium afterhyperpolarization of hypoglossal motoneurons in a rat brain stem slice preparation. *J Neurophysiol* 83: 2987-2995, 2000.

Lasser-Ross N, Ross WN, and Yarom Y. Activity-dependent [Ca2+]i changes in guinea pig vagal motoneurons: relationship to the slow afterhyperpolarization. *J Neurophysiol* 78: 825-834, 1997.

Lee RH and Heckman CJ. Bistability in spinal motoneurons in vivo: systematic variations in persistent inward currents. *J Neurophysiol* 80: 583-593, 1998a.

Lee RH and Heckman CJ. Bistability in spinal motoneurons in vivo: systematic variations in rhythmic firing patterns. *J Neurophysiol* 80: 572-582, 1998b.

Lee RH and Heckman CJ. Enhancement of bistability in spinal motoneurons in vivo by the noradrenergic alpha1 agonist methoxamine. *J Neurophysiol* 81: 2164-2174, 1999.

Lee RJ, Shaw T, Sandquist M, and Partridge LD. Mechanism of action of the non-steroidal anti-inflammatory drug flufenamate on [Ca2+]i and Ca(2+)-activated currents in neurons. *Cell Calcium* 19: 431-438, 1996.

Li Y and Bennett DJ. Persistent sodium and calcium currents cause plateau potentials in motoneurons of chronic spinal rats. *J Neurophysiol* 90: 857-869, 2003.

Li Y, Gorassini MA, and Bennett DJ. Role of persistent sodium and calcium currents in motoneuron firing and spasticity in chronic spinal rats. *J Neurophysiol* 91: 767-783, 2004a.

Li Y, Harvey PJ, and Bennett DJ. Spastic long-lasting reflexes in the chronic spinal rat, studied in vitro. *J Neurophysiol* 91: 2236-2246, 2004b.

Lipscombe D, Helton TD, and Xu W. L-type calcium channels: the low down. *J Neurophysiol* 92: 2633-2641, 2004.

Maxwell L, Maxwell DJ, Neilson M, and Kerr R. A confocal microscopic survey of serotoninergic axons in the lumbar spinal cord of the rat: co-localization with glutamate decarboxylase and neuropeptides. *Neuroscience* 75: 471-480, 1996.

McCarthy RT and TanPiengco PE. Multiple types of high-threshold calcium channels in rabbit sensory neurons: high-affinity block of neuronal L-type by nimodipine. *J Neurosci* 12: 2225-2234, 1992.

McLarnon JG. Potassium currents in motoneurones. *Prog Neurobiol* 47: 513-531, 1995.

Oomura Y and Maeno T. Does the neurone soma actually generate action potentials? *Nature* 197: 358-359, 1963.

Patel R, Kerr R, and Maxwell DJ. Absence of co-localized glutamic acid decarboxylase and neuropeptides in noradrenergic axons of the rat spinal cord. *Brain Res* 749: 164-169, 1997.

Perrier JF, Alaburda A, and Hounsgaard J. Spinal plasticity mediated by postsynaptic L-type Ca2+ channels. *Brain Res Brain Res Rev* 40: 223-229, 2002.

Perrier JF and Hounsgaard J. 5-HT2 receptors promote plateau potentials in turtle spinal motoneurons by facilitating an L-type calcium current. *J Neurophysiol* 89: 954-959, 2003.

Perrier JF and Hounsgaard J. Ca(2+)-activated nonselective cationic current (I(CAN)) in turtle motoneurons. *J Neurophysiol* 82: 730-735, 1999.

Pineda JC, Galarraga E, and Foehring RC. Different Ca2+ source for slow AHP in completely adapting and repetitive firing pyramidal neurons. *Neuroreport* 10: 1951-1956, 1999.

Pineda JC, Waters RS, and Foehring RC. Specificity in the interaction of HVA Ca2+ channel types with Ca2+-dependent AHPs and firing behavior in neocortical pyramidal neurons. *J Neurophysiol* 79: 2522-2534, 1998.

Powers RK and Binder MD. Persistent sodium and calcium currents in rat hypoglossal motoneurons. *J Neurophysiol* 89: 615-624, 2003.

Purvis LK and Butera RJ. Ionic current model of a hypoglossal motoneuron. *J Neurophysiol* 93: 723-733, 2005.Schwindt PC and Crill WE. Factors influencing

motoneuron rhythmic firing: results from a voltage-clamp study. *J Neurophysiol* 48: 875-890, 1982.

Schwindt PC and Crill WE. Properties of a persistent inward current in normal and TEA-injected motoneurons. *J Neurophysiol* 43: 1700-1724, 1980.

Schwindt PC, Spain WJ, Foehring RC, Stafstrom CE, Chubb MC, and Crill WE. Multiple potassium conductances and their functions in neurons from cat sensorimotor cortex in vitro. *J Neurophysiol* 59: 424-449, 1988.

Simon M, Perrier JF, and Hounsgaard J. Subcellular distribution of L-type Ca2+ channels responsible for plateau potentials in motoneurons from the lumbar spinal cord of the turtle. *Eur J Neurosci* 18: 258-266, 2003.

Stein RB, Bobet J, Oguztoreli MN, and Fryer M. The kinetics relating calcium and force in skeletal muscle. *Biophys J* 54: 705-717, 1988.

Svirskis G and Hounsgaard J. Depolarization-induced facilitation of a plateau-generating current in ventral horn neurons in the turtle spinal cord. *J Neurophysiol* 78: 1740-1742, 1997.

Svirskis G and Hounsgaard J. Transmitter regulation of plateau properties in turtle motoneurons. *J Neurophysiol* 79: 45-50, 1998.

Tombaugh GC, Rowe WB, and Rose GM. The slow afterhyperpolarization in hippocampal CA1 neurons covaries with spatial learning ability in aged Fisher 344 rats. *J Neurosci* 25: 2609-2616, 2005.

Umemiya M and Berger AJ. Properties and function of low- and high-voltage-activated Ca2+ channels in hypoglossal motoneurons. *J Neurosci* 14: 5652-5660, 1994.

Viana F, Bayliss DA, and Berger AJ. Multiple potassium conductances and their role in action potential repolarization and repetitive firing behavior of neonatal rat hypoglossal motoneurons. *J Neurophysiol* 69: 2150-2163, 1993.

Williams S, Serafin M, Muhlethaler M, and Bernheim L. Distinct contributions of high- and low-voltage-activated calcium currents to afterhyperpolarizations in cholinergic nucleus basalis neurons of the guinea pig. *J Neurosci* 17: 7307-7315, 1997.

Wu Y and Anderson ME. Ca2+-activated non-selective cation current in rabbit ventricular myocytes. *J Physiol* 522 Pt 1: 51-57, 2000.

Xu W and Lipscombe D. Neuronal Ca(V)1.3alpha(1) L-type channels activate at relatively hyperpolarized membrane potentials and are incompletely inhibited by dihydropyridines. *J Neurosci* 21: 5944-5951, 2001.

Zong S, Zhou J, and Tanabe T. Molccular determinants of calcium-dependent inactivation in cardiac L-type calcium channels. *Biochem Biophys Res Commun* 201: 1117-1123, 1994.

Chapter 3: Persistent calcium currents in adult rat motoneurons are facilitated by serotonin, and become supersensitive to serotonin following long-term spinal cord injury

Introduction

A spasticity syndrome is often seen after central nervous system injury, featured as muscle hyperreflexia, hypertonus, clonus and spasms (Ashby et al. 1987; Bennett et al. 1999a; Heckman 1994; Taylor et al. 1997; Ward 2002). Recently, the motoneuron properties and ionic mechanisms underlying spasticity have been investigated. The results indicate that the intrinsic excitability of motoneurons is profoundly increased over the months following spinal cord injury, and plays a major role in the generation of spasticity, in both rats (Bennett et al. 2001a; Bennett et al. 2001b; Li et al. 2004a) and humans (Gorassini et al. 2004). That is, a brief stimulation can trigger long lasting firing by activating voltage-dependent persistent inward currents (PICs) on motoneurons, which can cause a sustained depolarization (plateau potential) and firing that outlasts the stimulation by many seconds. These PICs can be triggered by dorsal root stimulation, which in turn produces self-sustained firing in the motoneurons and thus play a major role in the long-lasting spastic reflexes seen after chronic spinal cord injury.

The PICs responsible for plateaus in motoneurons have been shown to be mediated by L-type calcium channels (Li and Bennett 2003; Perrier et al. 2002; Simon et al. 2003) and TTX-sensitive persistent sodium currents (Li and Bennett 2003). The Na PICs are activated sub-threshold, but partly inactivated over a few seconds. In contrast, the L-type calcium current (Ca PIC) can persist for many seconds and contributes to about 60% of the sustained depolarization (plateau). Following chronic spinal cord injury, there are dramatic changes in the Na and Ca PICs in motoneurons below the level of injury. These

PICs induce large rapidly activating plateaus that cause sustained muscle spasms (Bennett et al. 2001b; Li and Bennett 2003).

The ability to activate plateaus in normal motoneurons relies on the facilitation of PICs by neuromodulators including 5-HT and NE acting on 5-HT_2 and α_1-NE receptors on motoneurons (Harvey et al. 2005c; Lee and Heckman 1999; Perrier and Delgado-Lezama 2005; Perrier and Hounsgaard 2003). Following acute spinal cord transection, the PICs in motoneurons are small, and not sufficient to produce plateaus, due to the loss of brainstem-derived neuromodulators such as 5-HT and NE (Harvey et al. 2005a,b). However, motoneurons somehow regain the ability to spontaneously exhibit large Na and Ca PICs and plateaus over the months following the injury, even though they are completely isolated from the brainstem (Bennett et al. 2001b).

Recently, the origin of the large Na PICs in chronic spinal rats has been demonstrated to be due to small amounts of residual 5-HT and NE in the spinal cord, because 5-HT and NE receptor antagonists eliminate these Na PICs (Harvey et al. 2005c). Only 2-15% of normal 5-HT amounts remain below a chronic spinal transection (Hains et al. 2002; Newton and Hamill 1988), but motoneurons develop a supersensitivity to 5-HT that more than overcomes this reduction in normal 5-HT. That is, very small amounts of 5-HT (less than 1μM) facilitate Na PICs in chronic spinal rats, whereas much larger doses of 5-HT are needed in normal motoneurons (30μM; 30-fold supersensitivey) (Harvey et al. 2005b).

The objective of the present study was to determine whether a similar supersensitivity to 5-HT develop for the Ca PICs, like that described for the Na PICs. If so, this would explain why the Ca PIC is also large in chronic spinal rats. That is, residual 5-HT may act on supersensitive receptors to enhance Ca PICs and ultimately contribute to spasticity. Our results confirmed the supersensitivity of the Ca PICs to 5-HT after chronic injury. Interestingly, 5-HT not only increased the amplitude of the Ca PICs at very low doses, but it also dramatically lowered the onset threshold of the Ca PICs, making these persistent currents larger and easier to activate.

Methods

Intracellular recordings were made from motoneurons in the sacrocaudal spinal cord of both normal adult rats (female Sprague-Dawley; 3 – 8 months old, n = 9) and spastic adult rats with chronic spinal cord injury (3 – 8 months old, n = 11). The chronic spinal rats were transected at 2 months of age (adult rat) and recordings were made after their affected muscles became spastic (1 – 6 months after injury). See Bennett et al. (1999a) for details of the chronic spinal transection and spasticity assessment. All recordings were made from the whole sacrocaudal spinal cord that was removed from the rat with a S2 sacral transection and maintained *in vitro*. This transection was made in chronic spinal rats just rostral to the chronic spinal injury, so as not do further damage to the sacrocaudal cord. In contrast, in the normal rats, the spinal cord was necessarily acutely injured in the in vitro preparation (cut at S2), and thus we refer to these motoneurons as from acute spinal rats. Like in other in vitro slice or whole cord preparations, this acute injury produced the characteristic effects of spinal shock, where motoneurons were relatively unexcitable, compared to those of chronic spinal rats or normal intact animals (Bennett et al. 2001b). All experimental procedures were approved by the University of Alberta Health Sciences Animal Policy and Welfare Committee.

In vitro preparation

Details of the experiment procedures have been described in previous publications (Li et al. 2004a; Li et al. 2004b). Briefly, all the rats were anaesthetized with urethane (0.18 g/100 g; with a maximum dose of 0.45 g), and part of the caudal cord (between the T13 and L6 vertebrae) was exposed and kept wet with modified artificial cerebrospinal fluid (mACSF). The rat was given pure oxygen for 5 minutes and then the cord was removed and transferred to a dissection chamber containing mACSF. All spinal roots were removed carefully, except the S4 and Ca1 ventral roots. The cord was secured by gluing the dorsal surface of the cord onto a small piece of nappy paper. After an incubation of 1.5 hours in the dissection chamber at room temperature (20-21° C), the cord was transferred to a recording chamber containing normal artificial CSF (nACSF) maintained near 24° C and with a flow rate > 5 mL/min. The cord was fixed onto the bottom of the recording chamber with the ventral side up by pinning the nappy paper to the Sylgard base of the chamber. A one hour period in nACSF was given to wash out the residual anaesthetic and kynurenic acid, and then the nACSF was recylced as follows. The nACSF was oxygenated in a 200-mL source bottle, and then ran through the recording chamber. This nACSF running out of the recording chamber was collected, filtered and returned to the source bottle with a pump. Because of the large volume (200 mL) of the source bottle and the small volume of the cord (< 0.05 mL), any accumulation of possible metabolic byproducts was negligible.

Intracellular recording

Intracellular recording methods were as described in Li and Bennett (2003) and were briefly summarized here. Sharp intracellular electrodes were made from thick-walled glass

capillary tubes (1.5mm O.D.; Warner GC 150F-10) using a Sutter P-87 micropipette puller and filled with a mixture of 1M K-acetate and 1M KCl. Electrodes were bevelled down from an initial resistance of 40-80 MΩ to 25-30 MΩ using a rotary beveller (Sutter BV-10). A stepper-motor micromanipulator (660, Kopf) was used to advance the electrodes through the tissue and break into cells. The S4 and Ca1 ventral roots were wrapped around Ag/AgCl electrodes above the recording chamber and sealed with complex grease (Dow Corning Corp.), which allows for antidromic stimulation and thus used to identify motoneurons. A bead of Dow Corning high vacuum grease was put around the edge of the complex grease to stop possible droplets of the complex grease into the flow. Only motoneurons with resting potential below -60 mV and antidromic spike overshoot over 0mV were considered healthy and used for recording. We also recorded from motoneurons after TTX was applied to block all the sodium channels, though we could not directly identify these as motoneurons by antidromic stimulation, because of the block of the antidromic spike by TTX. However, we found that these neurons could be reliably identified as healthy motoneurons by their characteristic membrane properties and location (See chapter 2 for details). Data were collected with an Axoclamp 2b intracellular amplifier (Axon Instruments, Burlingame, CA) running in discontinuous current clamp (DCC, switching rate 5-8 kHz, output bandwidth 3.0 kHz) or discontinuous single-electrode voltage clamp (SEVC; gain 0.8 to 2.5 nA/mV) modes.

Drugs and solutions

Two kinds of artificial cerebrospinal fluid (ACSF) were used in these experiments; a modified ACSF (mACSF) in the dissection chamber prior to recording and a normal ACSF (nACSF) in the recording chamber. The mACSF was composed of (in mM) 118 NaCl, 24 $NaHCO_3$, 1.5 $CaCl_2$, 3 KCl, 5 $MgCl_2$, 1.4 NaH_2PO_4, 1.3 $MgSO_4$, 25 D-glucose and 1 kynurenic acid. Normal ACSF was composed of (in mM) 122 NaCl, 24 $NaHCO_3$, 2.5 $CaCl_2$, 3 KCl, 1 $MgCl_2$ and 12 D-glucose. Both types of ACSF were saturated with 95% O_2-5% CO_2 and maintained at pH 7.4. Additional drugs were added as required, including 2 μM tetrodotoxin (TTX; Alamone Labs, Israel), 0.15 μM apamin (Alamone Labs, Israel) and 1-50 μM 5-HT (Sigma). The spinal cords were briefly exposed to nACSF solution containing 0.04% pronase E (Helixx Technologies) for 10 seconds prior to recording to weaken the pia of the spinal cord and allow for easier penetration (Buschges 1994). The pronase E did not induce noticeable changes of the motoneuron properties.

Persistent inward currents in current and voltage clamp recording

Slow triangular current ramps (0.4 nA/s) were applied to the motoneurons to measure basic cell properties. The input resistance (Rm) was measured during the ramp over a 5-mV range near rest and subthreshold to PIC onset. The plateau potential was seen as a subthreshold acceleration in membrane potential prior to firing and a long after-depolarization. Bistable behaviour was quantified by measuring self-sustained plateau (ΔI): i.e., when the plateau continued at less current than was initially used to activate the plateau.

This was quantified by subtracting the current at offset from the current at the onset of the plateau.

Slow triangular voltage ramps (3.5 mV/s) were applied to measure the PICs in voltage clamp. During the upward portion of the ramp, the current initially increased linearly with voltage in response to the passive leak conductance. A linear relation was fit in this region (10 mV below the PIC onset) and extrapolated to the whole range of the ramp (leak current). At depolarized potential and the PIC onset threshold was reached, there was a steep downward deviation from the extrapolated leak current. The onset voltage for the PIC (V_{on}) was defined as the voltage at which the I-V slope first reached zero (Li and Bennett 2003). The amplitude of the PIC was measured as the peak amplitude of this downward deviation. Large PICs usually caused a negative slope in the current response. Smaller PICs only caused a downward deflection in the current response (flattening of I-V slope) without a negative-slope region. V_{on} is not possible to pick in cells without a negative-slope region. Similarly, the offset voltage for the PIC (V_{off}) was defined as the voltage at which the I-V slope reached zero on the downward ramp. The difference between V_{on} and V_{off} (V_{on}-V_{off}) was used to compute the hysteresis of the PIC. The currents corresponding to V_{on} and V_{off} are defined as I_{on} and I_{off} respectively. A linear current response, not deviating downward from the leak current line (linear I-V relation), was used to indicate the absence of any PIC. The width of the PIC (V_w) was defined as the span between V_{on} and the voltage at which the current reached I_{on} for the second time on the upward section during the ramp (defined as V_{jump}), that is, $V_w = V_{jump} - V_{on}$. Previously, it has been shown that the width of the PIC

corresponds to the amplitude of the plateau potential that can be produced by the PIC (Li and Bennett 2003).

The depth of the PIC is defined as the difference between Ion and the second zero-slope point on the ramp (the peak of the PIC, I_P). The spike voltage threshold (V_{th}), was averaged from five consecutive spikes starting with the second spike on the up ramp, and was taken as the voltage at which the rate of the membrane potential change (dV/dt) higher than 10V/s (Li et al. 2004a).

Data analysis

Data were analyzed in Clampfit 8.0 (Axon Instruments, USA), and figures were made in Sigmaplot (Jandel Scientific, USA). Data are shown as mean ± standard deviation. A Student's t-test was used to test for statistical differences, with a significance level of $P < 0.05$.

Results

Intracellular recordings were made from 11 motoneurons from chronic spinal rats and 9 motoneurons from acute spinal rats. As previously described (Harvey et al. 2005a), both of these groups of motoneurons exhibited Ca and Na PICs, though the Ca PIC were larger in the chronic spinal rats and we focus on these first.

L-Ca current in chronic spinal rats are large and produce plateaus

In the voltage-range below - 40mV, where the membrane potential spends most of its time even during firing, there are only two major persistent inward currents: the Na PIC and the Ca PIC. Application of TTX eliminates the Na PIC, leaving the Ca PIC in isolation (Li and Bennett, 2003). This isolated Ca PIC is composed of inward current flowing directly through the L-type calcium channels (L-Ca current; nimodipine-sensitive) and calcium-activated currents triggered by the L-Ca current. Recently, we have shown that the major calcium activated current in motoneurons is the apamin-sensitive calcium activated potassium current (SK current), which produces an outward current that opposes the L-Ca current (see chapter 2). Thus, to examine the L-Ca currents without complication from this SK current we applied apamin to block it. The resulting L-Ca current, measured in TTX and apamin, is shown in Fig 3-1A.

In motoneurons from chronic spinal rats, the L-Ca current was activated at on average – 56.7±6.0 mV (V_{on}) and produced a downward deflection in the current response to an increasing voltage, which was quantified by subtracting the current from the extrapolated subthreshold leak current (thin line in Fig 3-1B, see Methods). On average the initial peak of the L-Ca (length of arrow in Fig 3-1A) was 2.4±1.0 nA. Usually, the L-Ca current was large enough in chronic spinal rats to overcome the increasing leak current and produce an outright negative-slope region (NSR; labeled in Fig 3-1B), and the depth of this NSR was 1.51±0.8 nA (Table 3-1). Following the NSR the measured current increased again with increasing voltage, and only overcame the leak current (passing the onset current for the L-Ca current, Ion, 3.8±1.4nA), when the potential was on average – 46.5±7.0 mV greater than V_{on} (width of valley formed by NSR, termed V_w; Fig 3-1B). When the voltage was then decreased, there was a clearly sustained L-Ca current (sustained peak 1.7±1.1nA), which only turned off when the voltage was significantly below the onset voltage (V_{off} = -65.3±6.6mV). This hysteresis (V_{on} - V_{off}) is likely due to the dendritic currents involved in the L-Ca current, which are only poorly clamped by the voltage clamp that we applied at the soma (Lee and Heckman 1996). The L-Ca current was, as expected, blocked by the L-type calcium channel blocker nimodipine (15μM), or by the general calcium channel blocker cadmium (400μM).

PIC properties	Membrane potential (mV)	conductance (μS)	V_{on} (mV)	Amplitude of initial PIC (nA)	Amplitude of sustained PIC (nA)	Width of initial PIC (mV)	Depth of NSR (nA)
nACSF	-76.7±7.0	0.24±0.09	-56.7±6.0	2.4±1.0	1.69±1.1	10.2±6.2	1.51±0.8
low dose 5-HT	-67.7±7.3	0.13±0.03	-63.7±7.1	3.0±0.73	2.2±0.75	17.7±4.9	1.9±0.63

Table 3-1 Effects of 5-HT on motoneurons of chronic spinal rats

Functionally, the large L-Ca current in chronic spinal rats produced a plateau potential, when the membrane potential was free to change in current clamp mode (Fig 3-2A). That is, during an increasing current injection, this plateau started with the same threshold (V_{on}, I_{on}) as the L-Ca current itself, and had a height that was proportional to the width of the valley formed by the negative slope region (V_w). Also, it was terminated only by reducing the current well below the onset current (I_{on}).

The L-Ca current is resistant to long-term block of spike mediated transmission

As stated above the L-Ca current was studied in isolation from the sodium currents by applying TTX. A secondary advantage of applying TTX is that it blocks all spike-mediated synaptic inputs to the motoneurons. This indirect effect of TTX has previously been shown to only produce a small (20 %) reduction in the L-Ca current, likely via a reduction in transmitters that facilitate the L-Ca current (Li and Bennett, 2003). Indeed, in the presence of TTX we found that large L-Ca currents persisted for many hours (up to 4 hours tested, n = 5), indicating that whatever transmitters facilitate the L-Ca current (e.g. endogenous 5-HT, Harvey et al. 2005b), these are mostly not released in a spike mediated manner (TTX resistant; except for the transmitters involved in the 20% reduction of the L-Ca current by TTX).

Low dose of 5-HT facilitated the L-Ca current in chronic spinal rats

When a low dose of 5-HT (1μM) was applied to motoneurons of chronic spinal rats the L-Ca current was dramatically altered in its onset threshold, duration/width and amplitude (n=11) (Fig 3-1B&3-2D), all of which led to markedly enhanced plateaus (Fig 3-2C) and thus greater overall excitability of motoneurons. This occurred despite the presence of TTX to block transmission, so the effects of 5-HT must have been directly on the motoneurons themselves, and not by indirect effects on interneurons. Specifically, the onset threshold of the L-Ca current was decreased significantly by 7.0±4.7 mV, and the width of the valley formed by this current was significantly increased by 7.5±3.7 mV. Further, the amplitude of the PIC was also significantly increased, in both its initial and sustained peaks. This led to a greater NSR, with a depth also significantly larger (see Table 3-1).

Together, with these changes in the L-Ca current, the resting membrane potential and input conductance (Gm) were both significantly reduced by the low dose of 5-HT. This is consistent with previous reports (Harvey et al. 2005a).

Interaction of 5-HT-induced changes in input conductance and L-Ca current

Interestingly, with 5-HT the onset voltage (V_{on}) was lowered more than the offset voltage (V_{off}), so the amount of hysteresis (V_{off} - V_{on}) was significantly reduced, though not eliminated by 5-HT. It is possible that this reduction in hysteresis might be in part related to the decreased conductance, which could make dendritic L-Ca currents more readily activated and clamped. However, we found no significant correlation between the

change in conductance and change hysteresis with 5-HT application (r = 0.48, n=11). Likewise, there was no significant correlation between the 5-HT-induced change in conductance and the change in PIC width (V_w, r = 0.29), onset voltage (V_{on}, r = 0.18) or amplitude (r = 0.47). Thus, the 5-HT induced change in input conductance cannot trivially account for the dramatic changes in PIC observed.

The 5-HT-induced L-Ca current is ultra long lasting after removal of 5-HT

Following 5-HT application the changes in the L-Ca current took about 10 - 15 minutes to reach a peak, and after that remained stable while in 5-HT. So the L-Ca current is only slowly modulated by 5-HT and does not habituate. Furthermore, after removal of 5-HT from the bath the L-Ca current was not immediately reduced, and remarkably it instead *increased* for about 45 min (significant increase of 0.51±0.1 nA, n=6). Following this paradoxical increase, the L-Ca current slowly decreased, but even 2 hrs after washout was still significantly greater than control conditions. We were not able to hold cells longer than this to evaluate full washout and reversal of the effects of 5-HT. It suffices to say that the effect of 5-HT on the Ca PIC must be ultra long lasting (similar slow action of 5-HT was seen in acute spinal rats, described below). For comparison, the changes in membrane potential and input resistance, induced by 5-HT were reversed within 15 - 20 minutes of removal of 5-HT (see Harvey et al. 2005a), so 5-HT receptor activation was indeed terminated by washing 5-HT from the bath. Somehow, the receptor or intracellular path involved in controlling the L-Ca current must be different and much longer lasting than that controlling the Rm and Vm. This receptor/pathway must also be different than

the receptor that controls the Na PIC, because the effects of 5-HT on the Na PIC are reversed within 45 minutes of removal of 5-HT (Harvey et al. 2005b).

Higher 5-HT doses in chronic spinal rats had no further effect

Higher doses of 5-HT (10-30μM) had similar effects to the standard low dose (1μM) described above (6 out 6 motoneurons tested), as shown in Fig 3-3C. In particular, the L-Ca onset (V_{on}), amplitude and width were not significantly increased by high dose 5-HT compared to in low dose 5-HT. Likewise, the hysteresis and width of the PIC were also not significantly different with high and low dose 5-HT, nor was the input conductance different. Thus, the low 1μM dose appears to provide a maximal effect on the L-Ca current in chronic spinal rats, similar to that described for 5-HT induced changes in the Na PIC in motoneurons (Harvey et al. 2005b).

The L-Ca current is supersensitive to 5-HT in chronic compared to acute spinal rats

In contrast to in chronic spinal rats, the low dose of 5-HT (1μM) had no significant effect on the L-Ca current or other motoneuron properties in acute spinal rats (n=5) (Fig 3-4B). A much higher dose of 5-HT (10 – 50 μM) was needed to induce similar changes in the L-Ca current in acute spinal rats as seen in chronic spinal rats for low doses (n=9) (Fig 3-4C). For many of the motoneurons from acute spinal rats, there is no NSR and high dose 5-HT usually increased the L-Ca enough to produce a NSR (as in Fig 3-5). The onset

threshold was significantly reduced and the PIC amplitude significantly increased by this high dose (Table 3-2). The 5-HT induced increase in PIC was similar in absolute value to in chronic spinal rats, but because the PICs in acute spinal rats were initially much smaller, 5-HT had a greater relative effect, nearly doubling the small PICs seen in acute spinal rats, and bringing them closer to the PICs seen in chronic spinal rats (prior to 5-HT). Because many acute spinal motoneurons had such small PICs initially (see above), there was not a NSR and the width of the PIC was impossible to quantify, and thus these parameters were not measured prior to 5-HT.

PIC properties	Membrane potential (mV)	conductance (μS)	V_{on} (mV)	Amplitude of initial PIC (nA)	Amplitude of sustained PIC (nA)	Width of initial PIC (mV)	Depth of NSR (nA)
nACSF	-77.9±7.8	0.28±0.09	-58.5±14.8	0.69±1.05	0.62±1.05	N/A	N/A
High dose 5-HT	-72.3±8.1	0.22±0.07	-62.5±3.6	1.27±1.1	1.1±1.1	7.4±5.0	0.41±0.5

Table 3-2 Effects of 5-HT on motoneurons of acute spinal rats

A high dose of 5-HT (10 - 50 μM) also significantly reduced the input conductance and depolarized the motoneurons (Table 3-2), whereas again, a low dose not effect these parameters in acute spinal rats.

In summary, the L-Ca current, input conductance and resting membrane potential are all supersensitive to 5-HT in motoneurons of chronic spinal rats, compared to in normal motoneurons in acute spinal rats (acutely isolated normal spinal cord). Up to 30 times

more 5-HT is required in acute spinal rats to have the same effect as in chronic spinal rats, indicating an approximately 30-fold supersensitivity in chronic spinal rats.

Discussion

5-HT increases persistent calcium currents, and lowers their threshold

Our results demonstrate that the low-voltage-activated persistent calcium current (L-Ca current) in adult rat motoneurons is facilitated by 5-HT, with a marked reduction in threshold and increase in amplitude. This produces a larger and wider negative-slope region in the I-V relation, which ultimately enhances (or enables) plateau potentials, making them larger in amplitude and lower in threshold. These results are consistent with previous reports of increases in the L-Ca current and Ca plateau with 5-HT (in turtle; Perrier and Hounsgaard 2003), though the marked reduction in the onset threshold had not previously been described.

Functionally, the lower threshold of the L-Ca current helps to enable activation during firing

Functionally, a reduction in the L-Ca threshold is as important as the increase in amplitude, because only the portion of the L-Ca current that is below the firing threshold voltage (V_{th}; about - 50 mV) can be activated during firing, because between spikes the AHP holds the potential below the firing threshold, and the L-Ca current is much too slow to respond to the couples of milliseconds depolarization during the spike (Li et al. 2004a). The L-Ca current that is activated during firing aides in sustaining firing, and enables self-sustained firing (firing that out lasts a stimulation; Li et al. 2004a). When the

L-Ca onset is well below the firing threshold, self-sustained firing is pronounced, and easily triggered (Li et al. 2004a). On the other extreme, when the L-Ca current is well above the firing threshold, it cannot be activated and does not produced self-sustained firing (Li et al. 2004a). Thus, by lowering the onset voltage of the PIC, 5-HT should enable the L-Ca current to be more fully activated during firing, and encourage self-sustained firing. This is often the case (Harvey et al. 2005a,b).

However, there are some cells that paradoxically become less excitable in 5-HT, with less self-sustained firing (Harvey et al. 2005a; Perrier and Hounsgaard 2003). This paradox partly arises because 5-HT also lowers the firing threshold, V_{th} (Harvey et al. 2005a; Fedirchuk and Dai 2004). So when this reduction in V_{th} exceeds the reduction in the onset voltage of the L-Ca current, V_{on}, then the L-Ca current is less able to activate during firing ($\Delta V_{th} > \Delta V_{on}$; Harvey et al. 2005a,b). Furthermore, the facilitation of the L-Ca current by 5-HT seems to work by the 5-HT_2 receptor class (Perrier and Hounsgaard 2003), whereas there may be an inhibition of the L-Ca current by 5-HT_{1A} receptors (Harvey and Bennett, unpublished data). Also, 5-HT has different effects on different spatial locations in the motoneurons (Perrier and Hounsgaard 2003). Thus, the balance of 5-HT_2 and 5-HT_{1A} activation and spatial distribution of the 5-HT innervation may determine whether 5-HT has a net facilitory affect on firing.

The facilitation of the L-Ca current by 5-HT is ultra long lasting

The results also demonstrate that not only does 5-HT facilitate the L-Ca currents, but these effects are very long lasting, continuing for as long as 5-HT is present, and not reversing for hours after removal of 5-HT. Unexpectedly, during the first 45 minutes after removal of 5-HT the L-Ca current tends to increase further, rather than decrease, though this is consistent with the recent findings that 5-HT-induced facilitation of spinal reflexes is further augmented after removal of 5-HT agonists (Machacek et al. 2001). Reversal of the effect of 5-HT receptor agonists on the L-Ca current (Results) and spinal reflexes (Machacek et al. 2001) takes many hours. Functionally, this leads to the surprising conclusion that normal 5-HT innervation of motoneurons, for example through transient raphe activation, should increase motoneuron excitability for many hours. Perhaps, 5-HT_{1A} receptors or other inhibitory coupled receptors, are able to rapidly inhibit the L-Ca currents (unpublished findings), and enable more fine minute-by-minute control of the motoneuron excitability. Furthermore, other actions of 5-HT, such as its depolarization and increase in input resistance are much more rapid to reverse than its action on the L-Ca current.

Origins of spontaneously occurring L-Ca currents

Because of the ultra long-lasting effects of 5-HT, the spontaneously occurring L-Ca currents that we measure in our in vitro spinal cord preparation could, in principle, be a result of 5-HT activation of motoneurons from the brainstem that occurs *at or before* the removal of the spinal cord from the animal. However, this is unlikely to be the case, because we do not observe a rundown of L-Ca currents many hours after removal of the

spinal cord from normal rats, when the 5-HT effects should be slowly reversed. Furthermore, in chronic spinal rats the brainstem innevation is completely gone months before the experiment, and thus cannot be involved.

In chronic spinal rats transmitters intrinsic to the spinal cord, including the residual amounts of 5-HT and NE in the chronic spinal animal (Newton and Hamill 1988), could in principle be responsible for enabling the large L-Ca currents seen in these animals. These transmitters, may be in small part be released by a spike-mediated manner, because there is on average a somewhat larger cadmium sensitive L-Ca current (20% larger) before compared to after a block of spike mediated transmission with TTX (Li et al. 2004a). However, the bulk of the L-Ca current persists in TTX, and even 3 - 5 hours after application of TTX large L-Ca currents can be observed (see results), suggesting that what ever transmitter facilitates the L-Ca current leaks from its terminal in a non-spike mediated manner.

L-Ca currents are supersensitive to 5-HT in chronic spinal rats and likely lead to large PICs

Following chronic spinal cord injury most of the 5-HT axons that innervate the spinal cord degenerate, because they arise from the brainstem (Maxwell et al. 1996). Nevertheless, there is about 2 - 15 % of the normal levels of 5-HT remaining below an injury site in a chronic spinal animal, in part due to intrinsic spinal 5-HT neurons, which can be fairly plastic following injury (Branchereau et al. 2002; Newton and Hamill 1988). The reduced 5-HT following injury is associated with a classic denervation

supersensitivity, because spinal reflexes are facilitated by unusually low doses of 5-HT (Bedard et al. 1979; Bedard et al. 1987). Further, many motoneuron parameters, including the input resistance, resting potential, persistent sodium current and L-Ca current become supersensitive to 5-HT (Results and Harvey et al. 2005b). Thus, the small amounts of residual 5-HT may have large effects on the motoneurons and reflexes and ultimately lead to the hyperexcitable state of chronic spinal animal. Indeed, recently it has been shown that both 5-HT and NE do leak from spinal sources in the chronic spinal rats to produce large persistent sodium currents seen in these motoneurons. This was primarily demonstrated by showing that blocking the action of these monoamines with 5-HT_2 and NE-α1 receptor antagonist eliminates these sodium currents (Harvey et al. 2005c). This elimination of these persistent sodium currents takes about 1 hour, similar to the time to reverse the effects of 5-HT on the sodium currents after removing 5-HT. The ultra long-lasting effects of 5-HT on the L-Ca current (hours) make similar experiments very difficult, though it is clear that endogenous 5-HT and NE are present and thus should be involved in enabling the large L-Ca currents seen in chronic spinal rats.

Summary and role of 5-HT in spasticity

The supersensitivity of the L-Ca current to 5-HT has important implications for the understanding of spasticity. Previously, it has been show that L-Ca currents produce the many second long spasms that are the hallmark of spasticity following spinal cord injury (Gorassini et al. 2004; Li et al. 2004a). Thus, the small amounts of endogenous 5-HT

below the injury in a chronic spinal rat likely act on supersensitive receptors to produce large L-Ca currents and ultimately enable muscle spasms. Furthermore, because the spinal sources of 5-HT are closely associated with the autonomic system, the L-Ca currents and spasms might be modulated with autonomic input, and for example help explain why bladder irritation or infection can lead to increased spasms in spinal cord injured patients (Knutsdottir 1993). Ultimately, understanding and treating spasticity will involve determining what 5-HT receptors are involved in facilitating the L-Ca current and what makes these receptors supersensitive. Our preliminary results suggest that 5-HT_{2B} receptors play a major role (Li and Bennett, unpublished results), consistent with the novel role 5-HT_{2B} receptors in modulating the reflexes involving L-type calcium channels in frog motoneurons (Holohean and Hackman 2004), and different from the 5-$HT_{2A/C}$ receptors that facilitate the persistent sodium current (Harvey et al. 2005c).

Figure 3-1

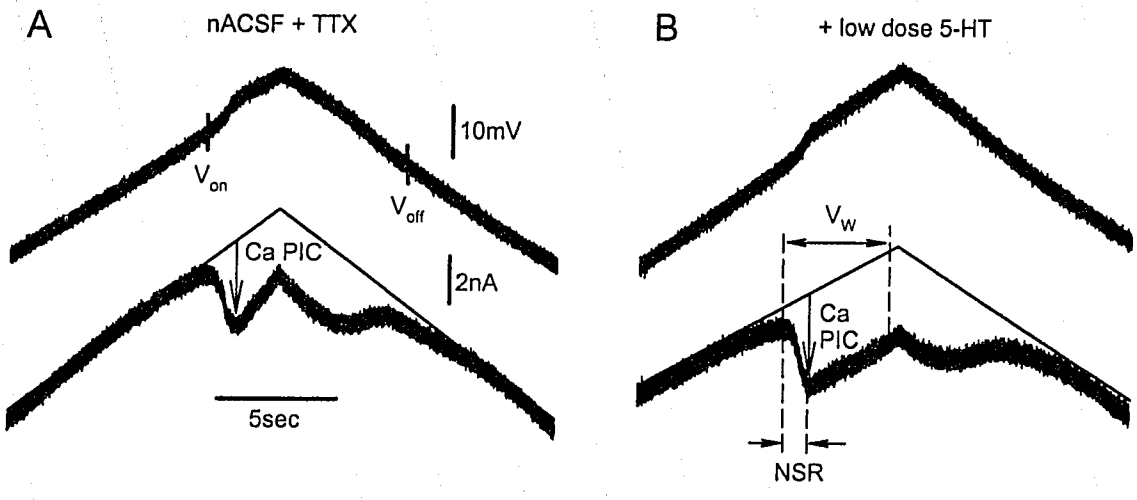

Figure 3-1. An example of low dose 5-HT facilitates Ca PIC in motoneurons from chronic spinal rats. A: shows a recording in voltage clamp mode prior to 5-HT. B: Low dose 5-HT lowered the Ca threshold, increased the PIC and lowered the conductance as predicted.

Figure 3-2

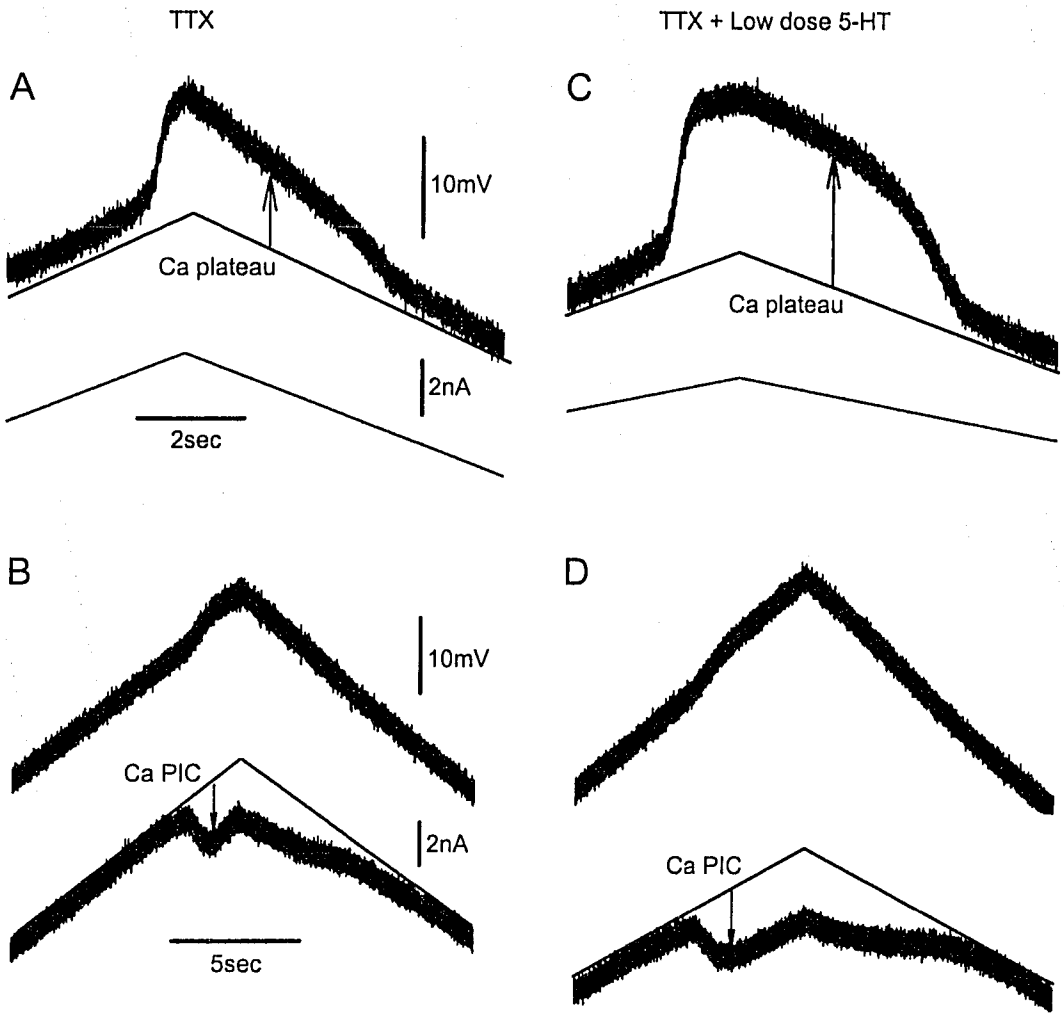

Figure 3-2. Another example of low dose 5-HT facilitates Ca PIC in motoneurons from chronic spinal rats. A: Ca plateau potential induced by increasing current ramp. B: A corresponding Ca PIC induced in voltage ramp mode, recorded from the same cell. C: Low dose 5-HT increased the Ca plateau significantly. D: Low dose 5-HT demonstrated complicated effects on the cell.

Figure 3-3

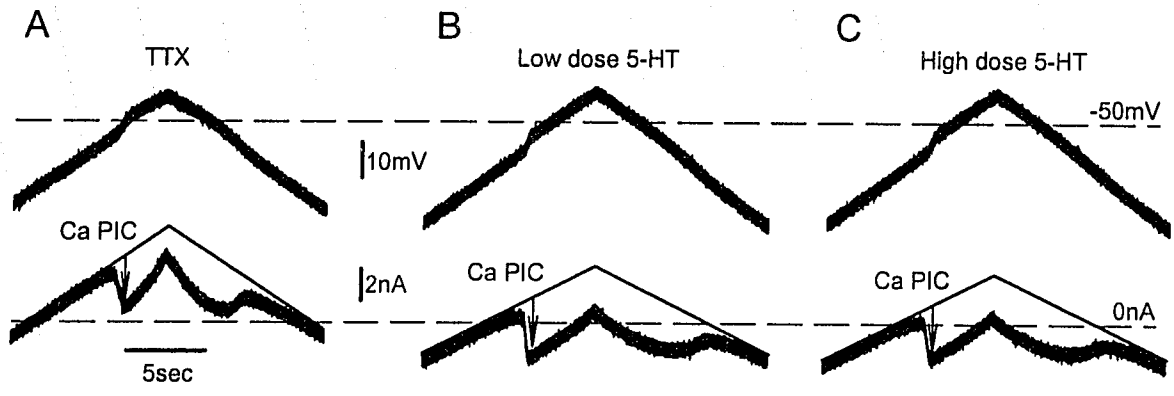

Figure 3-3. High dose 5-HT showed no further effects. A: A Ca PIC was induced in voltage clamp mode, recorded from a motoneuron from chronic spinal rats. B: Low dose 5-HT exhibited complicated effects on the cell. C: The effects of low dose 5-HT is almost saturated and high dose 5-HT showed no further effects.

Figure 3-4

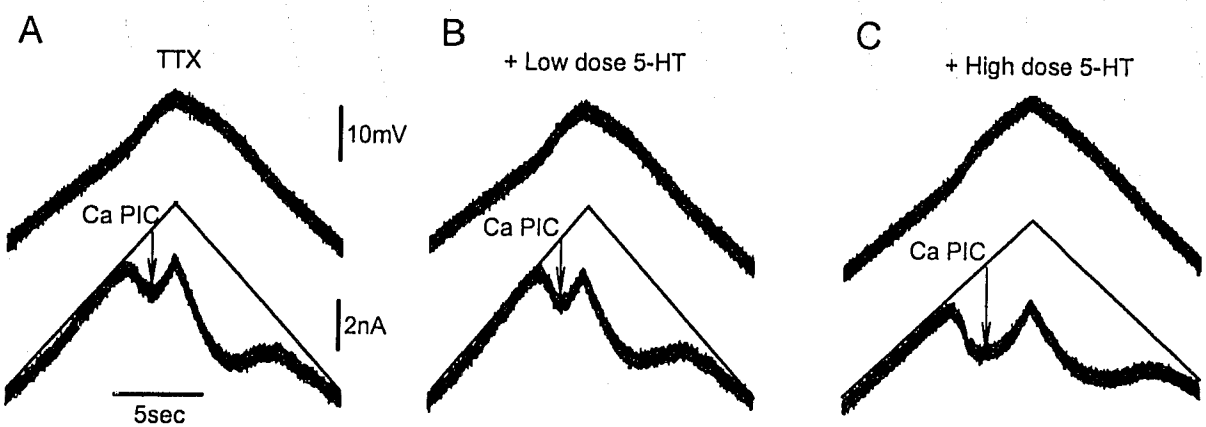

Figure 3-4. In acute motoneurons, high dose, but not low dose 5-HT facilitates Ca PIC. A: A Ca PIC was induced in voltage clamp mode. B: Low dose 5-HT showed no significant effects on the cell. C: High dose 5-HT exhibited comprehensive effects, lowered the Ca threshold, increased the PIC and lowered the conductance as predicted.

Figure 3-5

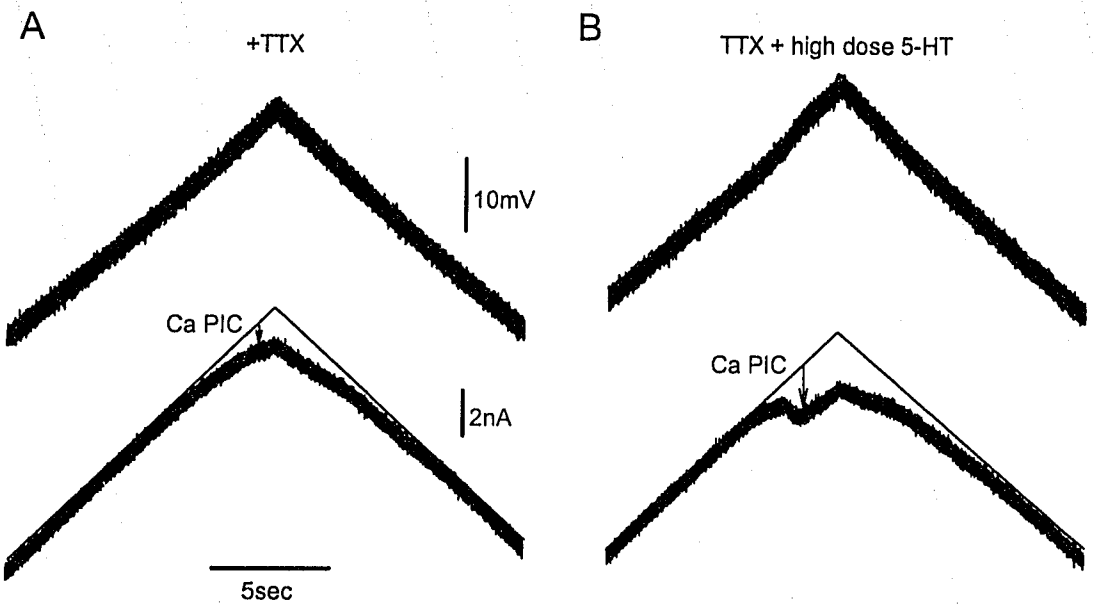

Figure 3-5. Another example of high dose 5-HT facilitates Ca PIC in acute motoneurons. A: Like in many of the acute motoneurons, a Ca PIC was induced by an increasing voltage ramp, but not sufficient to induce a NSR. B: High dose 5-HT lower the conductance and induced a bigger Ca PIC and a NSR.

References

Ashby P, Mailis A, and Hunter J. The evaluation of "spasticity". *Can J Neurol Sci* 14: 497-500, 1987.

Bedard P, Barbeau H, Barbeau G, and Filion M. Progressive increase of motor activity induced by 5-HTP in the rat below a complete secretion of the spinal cord. *Brain Res* 169: 393-397, 1979.

Bedard PJ, Tremblay LE, Barbeau H, Filion M, Maheux R, Richards CL, and DiPaolo T. Action of 5-hydroxytryptamine, substance P, thyrotropin-releasing hormone and clonidine on motoneurone excitability. *Can J Neurol Sci* 14: 506-509, 1987.

Bennett DJ, Gorassini M, Fouad K, Sanelli L, Han Y, and Cheng J. Spasticity in rats with sacral spinal cord injury. *J Neurotrauma* 16: 69-84, 1999.

Bennett DJ, Li Y, Harvey PJ, and Gorassini M. Evidence for plateau potentials in tail motoneurons of awake chronic spinal rats with spasticity. *J Neurophysiol* 86: 1972-1982, 2001a.

Bennett DJ, Li Y, and Siu M. Plateau potentials in sacrocaudal motoneurons of chronic spinal rats, recorded in vitro. *J Neurophysiol* 86: 1955-1971, 2001b.

Branchereau P, Chapron J, and Meyrand P. Descending 5-hydroxytryptamine raphe inputs repress the expression of serotonergic neurons and slow the maturation of inhibitory systems in mouse embryonic spinal cord. *J Neurosci* 22: 2598-2606, 2002.

Buschges A. The Physiology of Sensory Cells in the Ventral Scoloparium of the Stick Insect Femoral Chordotonal Organ. *J Exp Biol* 189: 285-292, 1994.

Fedirchuk B and Dai Y. Monoamines increase the excitability of spinal neurones in the neonatal rat by hyperpolarizing the threshold for action potential production. *J Physiol* 557: 355-361, 2004.

Gorassini M, Bennett D, and Yang JF. Excitability of motor units in persons with spasticity from spinal cord injury. *Soc Neurosci Abstr 25:120*, 1999.

Gorassini MA, Knash M, Harvey PJ, Bennett DJ, and Yang JF. Role of motoneuron plateau potentials in the generation of involuntary muscle activity after spinal cord injury. *Brain* 127: 2247-2258, 2004.

Hains BC, Everhart AW, Fullwood SD, and Hulsebosch CE. Changes in serotonin, serotonin transporter expression and serotonin denervation supersensitivity: involvement in chronic central pain after spinal hemisection in the rat. *Exp Neurol* 175: 347-362, 2002.

Harvey PJ, Li Y, Li X, and Bennett DJ. Persistent sodium currents and repetitive firing in motoneurons of the sacrocaudal spinal cord of adults. 2005. Submitted to J Neurophysiol.

Harvey PJ, Li Y, Li X, and Bennett DJ. Serotonin facilitates persistent sodium currents in motoneurons, and spinal cord transection leads to a supersensitivity to serotonin. 2005. Submitted to J Neurophysiol.

Harvey PJ, Li Y, Li X, and Bennett DJ. Endogenous monoamines are essential for persistent sodium currents and repetitive firing in rat spinal motoneurons. 2005. In preparation.

Heckman CJ. Alterations in synaptic input to motoneurons during partial spinal cord injury. *Med Sci Sports Exerc* 26: 1480-1490, 1994.

Holohean AM and Hackman JC. Mechanisms intrinsic to 5-HT2B receptor-induced potentiation of NMDA receptor responses in frog motoneurones. *Br J Pharmacol* 143: 351-360, 2004.

Hounsgaard J and Kiehn O. Serotonin-induced bistability of turtle motoneurones caused by a nifedipine-sensitive calcium plateau potential. *J Physiol* 414: 265-282, 1989.

Knutsdottir S. Spinal cord injuries in Iceland 1973-1989. A follow up study. *Paraplegia* 31: 68-72, 1993.

Lancaster B, Nicoll RA, and Perkel DJ. Calcium activates two types of potassium channels in rat hippocampal neurons in culture. *J Neurosci* 11: 23-30, 1991.

Lance JW and Burke D. Mechanisms of spasticity. *Arch Phys Med Rehabil* 55: 332-337, 1974.

Lasser-Ross N, Ross WN, and Yarom Y. Activity-dependent [Ca2+]i changes in guinea pig vagal motoneurons: relationship to the slow afterhyperpolarization. *J Neurophysiol* 78: 825-834, 1997.

Lee RH and Heckman CJ. Influence of voltage-sensitive dendritic conductances on bistable firing and effective synaptic current in cat spinal motoneurons in vivo. *J Neurophysiol* 76: 2107-2110, 1996.

Li Y and Bennett DJ. Persistent sodium and calcium currents cause plateau potentials in motoneurons of chronic spinal rats. *J Neurophysiol* 90: 857-869, 2003.

Li Y, Gorassini MA, and Bennett DJ. Role of persistent sodium and calcium currents in motoneuron firing and spasticity in chronic spinal rats. *J Neurophysiol* 91: 767-783, 2004a.

Li Y, Li X, Harvey PJ, and Bennett DJ. Effects of baclofen on spinal reflexes and persistent inward currents in motoneurons of chronic spinal rats with spasticity. *J Neurophysiol* 92: 2694-2703, 2004b.

Machacek DW, Garraway SM, Shay BL, and Hochman S. Serotonin 5-HT(2) receptor activation induces a long-lasting amplification of spinal reflex actions in the rat. *J Physiol* 537: 201-207, 2001.

Maxwell L, Maxwell DJ, Neilson M, and Kerr R. A confocal microscopic survey of serotoninergic axons in the lumbar spinal cord of the rat: co-localization with glutamate decarboxylase and neuropeptides. *Neuroscience* 75: 471-480, 1996.

Newton BW and Hamill RW. The morphology and distribution of rat serotoninergic intraspinal neurons: an immunohistochemical study. *Brain Res Bull* 20: 349-360, 1988.

Patel R, Kerr R, and Maxwell DJ. Absence of co-localized glutamic acid decarboxylase and neuropeptides in noradrenergic axons of the rat spinal cord. *Brain Res* 749: 164-169, 1997.

Perrier JF, Alaburda A, and Hounsgaard J. Spinal plasticity mediated by postsynaptic L-type Ca2+ channels. *Brain Res Brain Res Rev* 40: 223-229, 2002.

Perrier JF and Delgado-Lezama R. Synaptic release of serotonin induced by stimulation of the raphe nucleus promotes plateau potentials in spinal motoneurons of the adult turtle. *J Neurosci* 25: 7993-7999, 2005.

Perrier JF and Hounsgaard J. 5-HT2 receptors promote plateau potentials in turtle spinal motoneurons by facilitating an L-type calcium current. *J Neurophysiol* 89: 954-959, 2003.

Simon M, Perrier JF, and Hounsgaard J. Subcellular distribution of L-type Ca2+ channels responsible for plateau potentials in motoneurons from the lumbar spinal cord of the turtle. *Eur J Neurosci* 18: 258-266, 2003.

Taylor JS, Friedman RF, Munson JB, and Vierck CJ, Jr. Stretch hyperreflexia of triceps surae muscles in the conscious cat after dorsolateral spinal lesions. *J Neurosci* 17: 5004-5015, 1997.

Ward AB. A summary of spasticity management--a treatment algorithm. *Eur J Neurol* 9 Suppl 1: 48-52; dicussion 53-61, 2002.

Chapter 4: Conclusion

Present Results

In this thesis, we first hypothesized that the L-Ca (Cav1.3) PIC underlying the plateau potential activates an SK current, and this SK current ultimately counteracts the L-Ca PIC and makes the recorded net calcium PIC smaller. The second hypothesis was that the calcium channels responsible for the Ca PIC become supersensitive to 5-HT, and the supersensitivity of the channels to this endogenous 5-HT causes the large Ca PICs found in the motoneurons from chronic spinal rats. The results of our studies supported these hypotheses. It was demonstrated that:

1. The SK current responsible for the mAHP is activated by N-type or P/Q-type calcium current, but not by L-type calcium currents during the spikes.
2. The L-type Ca PIC (Cav1.3) does activate an SK current, which subsequently counteracts the L-Ca PIC.
3. The amplitudes of this L-type calcium current are not significantly different in motoneurons from chronic spinal rats than that from acute rats.
4. This L-type calcium current activated SK current is important for controlling the large L-Ca PICs that occur in motoneurons.
5. 5-HT makes motoneurons more excitable by depolarizing the membrane potential, decreasing the conductance of the cell, lowering the threshold of the Ca PIC and increasing the amplitude of the Ca PIC. This ultimately leads to larger, more easily activated plateaus and self-sustained firing.

6. After chronic spinal transection, the effects of 5-HT on motoneurons become 30-fold supersensitive to 5-HT, with 30 times the 5-HT concentration needed to facilitated Ca PICs and plateaus in normal rats compared to in chronic spinal rats. .

These results help explain the mechanism by which large PICs develop after spinal cord injuries and ultimately leads to the spasticity in patients. That is, residual 5-HT in the spinal cord below the spinal cord injury can act on supersensitive receptors to produce large Ca PICs, as has also been demonstrated for Na PICs (Harvey et al. 2005a). The results also show the interaction between the L-Ca PIC underlying the plateau potentials and the SK current activated by this low threshold L-Ca current, where the SK current essentially keeps the L-Ca current in check, so that it can be turned off.

Future Directions

Though the calcium channels have been proved to be supersensitive to 5-HT after chronic injury, it is still unclear what receptors are involved in this modulation. Among the sub-type receptors of 5-HT, the 5-HT_{1A} and 5-HT_{2B} receptors are promising candidates for the modulation and this idea has been supported by our preliminary research (results not shown). We know from previous results that the Ca PIC persists in the presence of 5-HT2a, 5-HT2c and alpha1 NE antagonists, unlike the Na PIC (Harvey et al. 2005b). So it is likely that the Na and Ca PICs are mediated by different receptors. Also, the mechanism underlying the supersensitivity after chronic injury is still unknown;

possibilities include: changes in the number or structures of the receptors/channels or changes of the intracellular pathways that facilitate the Ca PIC. Future studies focused on these aspects would improve the understanding of the motoneuron properties after chronic spinal cord injury and ultimately be critical in determining new treatments for spasticity, because the Ca PIC on the motoneurons has been shown to play the major role in producing sustains muscle spasms (Li et al. 2004).

References

Harvey PJ, Li Y, Li X, and Bennett DJ. Serotonin facilitates persistent sodium currents in motoneurons, and spinal cord transection leads to a supersensitivity to serotonin. 2005. Submitted to *J Neurophysiol.*

Harvey PJ, Li Y, Li X, and Bennett DJ. Endogenous monoamines are essential for persistent sodium currents and repetitive firing in rat spinal motoneurons. 2005. In preparation.

Li Y, Gorassini MA, and Bennett DJ. Role of persistent sodium and calcium currents in motoneuron firing and spasticity in chronic spinal rats. *J Neurophysiol* 91: 767-783, 2004